

ORIGINAL RESEARCH ARTICLE

**Bradykinin mediates the association of collecting duct cells to form migratory colonies,
through B2 receptor activation[†]**

Running head: BK induces collecting duct cell association

**Edith del Valle Guaytima¹, Yamila Romina Brandán¹, Nicolás Octavio Favale^{2,3}, Bruno
Jaime Santacreu^{2,3}, Norma B. Sterin-Speziale², and María Gabriela Márquez^{1*}**

Affiliation

¹ Instituto de Investigaciones en Ciencias de la Salud Humana (IICSHUM), Universidad Nacional de La Rioja, Av. Luis Vernet 1000, (5300) La Rioja, ARGENTINA

² Instituto de Química y Físico-Química Biológica (IQUIFIB) -CONICET, Facultad de Farmacia y Bioquímica, Universidad de Buenos Aires, Junín 956, (C1113AAD) Buenos Aires, ARGENTINA

³ Cátedra de Biología Celular y Molecular, Departamento de Ciencias Biológicas, Facultad de Farmacia y Bioquímica, Universidad de Buenos Aires, Junín 956, (C1113AAD) Buenos Aires, ARGENTINA

Correspondence to: María Gabriela Márquez, Instituto de Investigaciones en Ciencias de la Salud Humana (IICSHUM), Universidad Nacional de La Rioja, Av. Luis Vernet 1000, (5300) La Rioja, ARGENTINA, Phone: 0054-380-4438683; E-mail: gmarquezenator@gmail.com

[†]This article has been accepted for publication and undergone full peer review but has not been through the copyediting, typesetting, pagination and proofreading process, which may lead to differences between this version and the Version of Record. Please cite this article as doi: [10.1002/jcp.26472]

Additional Supporting Information may be found in the online version of this article.

Received 24 April 2017; Revised 14 December 2017; Accepted 3 January 2018
Journal of Cellular Physiology
This article is protected by copyright. All rights reserved
DOI 10.1002/jcp.26472

Contract grant sponsor: National Council for Scientific and Technologic Research-CONICET;

Contract grant number: PIP-413, PIP-502.

Contract grant sponsor: National Agency for Scientific and Technologic Promotion; Contract grant number: PICT-1625

Contract grant sponsor: National University of La Rioja; Contract grant number: 27/A544, 27/A626, 27/A674

Abstract

It is known that bradykinin (BK) B2 receptor (B2R) is expressed in the collecting duct (CD) cells of the newborn rat kidney, but little is known about its role during early postnatal life. Therefore, we hypothesize that BK could participate in the mechanisms that mediate CD formation during the postnatal renal development. Performing primary cultures, combined with biochemical, immunocytochemical, and time-lapse analysis, we studied the role of BK in CD cell behaviour isolated from renal papilla of neonatal rats. A reverse relationship was observed between B2R expression and the degree of CD epithelial cell sheet maturation. BK stimulation induced CD cell association upon B2R activation. The lack of B2R expression in cells showing mature adherens junctions suggested that BK is mostly involved in early adhesive events, thus favouring the initial formation of CD during development. Time-lapse analysis revealed that BK induced a high protrusive activity of CD cells, denoted by ruffle formation and lamellipodia extension. PI3K was involved in the BK-induced CD cell-cell association and the acquisition of the migratory phenotype since, when inhibited, membrane ruffles and filopodia between cells diminished. Results indicate that the actions of BK mediated by PI3K activation were due to the downstream Akt and Rac pathways. This study, performed with CD cells that were not genetically manipulated, provides new experimental evidence supporting a novel role of BK in rat renal CD organization. Since B2R blockade results in abnormal tubular differentiation, our results contribute to better understanding the etiology of human congenital renal malformation and diseases. This article is protected by copyright. All rights reserved

Keywords: bradykinin; B2 receptor; collecting duct; renal papilla; PI3K

Introduction

Renal collecting ducts (CD) play an essential role in the control of fluid and electrolyte composition of the body. In mammals, the formation of the kidney begins when the ureteric bud (UB), a caudal branch of the mesonephric duct (Wolffian duct), invades the surrounding metanephric mesenchyme, and a mutual induction takes place. As a result, the UB epithelium undergoes branching morphogenesis to give rise to the CD system of the adult kidney, whereas the metanephric mesenchyme gives rise to the nephron (Aperia and Celsi, 1992; Dressler, 2006; Pohl et al., 2000; Saxen, 1987). In humans, nephrogenesis is completed *in utero* before week 36, whereas in rats, it is completed postnatally (Aperia and Celsi, 1992; Dodge, 1997; Márquez et al., 2002). In previous studies, we and others have demonstrated that, at birth, the rat kidney is very immature, and that all stages of renal glomerular and tubular development can be visualized in histological sections of the newborn rat kidney (Dodge, 1997; Márquez et al., 2002). We have also demonstrated that the postnatal maturation is different in various areas of the kidney (Kahane et al., 1995; Márquez et al., 2002) and that different cell types also show a different degree of proliferation in each kidney area. Tubular papillary cells stop dividing on postnatal day 10, meanwhile cortical and medullary tubular cells still proliferate until postnatal day 20 (Kahane et al., 1995; Márquez et al., 2002). For these reasons, rats are a suitable animal model to study renal developmental mechanisms since nephrogenic structures are still present in the postnatal kidney.

The renal kallikrein-kinin system is a well-known modulator of renal hemodynamics and urinary sodium excretion in the adult kidney (Roman et al., 1988; Siragy, 1993; Vio et al., 1992). Two types of serine proteases kallikreins exist in humans, plasma and tissue kallikrein. Plasma kallikrein is found exclusively in the circulating blood, while tissue kallikrein can be found in various tissues, such as pancreas, kidney, intestine and salivary glands (Schachter, 1979). The expression of tissue kallikrein is regulated during nephrogenesis, and is observed as early as S-shaped bodies phase (El-Dahr and Chao, 1992; Xiong et al., 1989). In humans and rodents, there are two types of kininogen,

the kallikrein substrate, high molecular weight (HMW) and low molecular weight (LMW) kininogen, both of which are differential splicing products of the same kininogen gene transcript (Kitamura et al., 1983). Tissue kallikrein cleaves LMW kininogen into Lys- bradykinin (Lys-BK) or kallidin, whereas HMW kininogen is cleaved by plasma kallikrein into BK (Proud et al., 1981). During early rat nephrogenesis, the main kinin-expressing segments are the terminal UB branches, and when nephrogenesis is completed, the distribution of kininogens assumes its classic adult pattern in the CD. It has been reported that LMW kininogen is highly expressed in newborn rats, with a stage-specific patterns that changes from the terminal branches of the UB to the CD as the nephrogenesis proceeds (El-Dahr et al, 1998), however, in rats, tissue kallikrein can only release BK from LMW kininogen (Alhenc-Gelas et al., 1981; Kato et al., 1985; Hagiwara et al., 1995). In addition, in the rat, it has been reported the release of Arg-BK instead Lys-BK, as a kallidin-like peptide (Hilgenfeldt et al., 2005). In developing kidneys, LMW kininogen is synthesized and stored in UB branches and the principle cells of CD (El-Dahr, 2004). The spatial proximity of distal tubule expressing tissue kallikrein with UB and CD principle cells, allows a regionally independent machinery to produce kinins from enzymatic cleavage of kininogen, so-called the renal kallikrein-kinin system. The main renal kinin synthesized under physiological conditions is BK which exerts its classical renal effects through the activation of its B2 receptor (B2R) and can act in a paracrine manner because of its short half-life (Schanstra et al., 1999). Plasma aminopeptidases can convert kallidin to BK by cleavage of the first N-terminal lysine residue, and carboxypeptidase M (kininase D) generates their des-Arg-derivatives, which are agonist of the B1 receptor. Whereas the B2R is widely expressed, the B1 receptor is mainly induced in a variety of pathologies related to inflammation (Schanstra et al., 1999). BK and kallidin are degraded into inactive peptide fragments by angiotensin converting enzyme (kininase II) (Schanstra et al., 1999). In newborn rat kidneys, B2R gene expression is highly activated, being 30- to 40-fold higher than in adult rat kidneys (El-Dahr et al., 1997; Yosipiv et al., 1997). Furthermore, the blockade of B2R results in renal hypoplasia and abnormal tubular differentiation during fetal life, inducing a reduction in kidney

DNA synthesis and in the kidney-to-body weight ratio during neonatal development, while it has no effect on renal growth in adult rats (Yosipiv et al., 1994, 1997). In newborn rats, B2R immunoreactivity is present in CD cells, in the upper limb of S-shaped bodies (precursors of connecting tubules), and in connecting tubules, but not in undifferentiated mesenchyme or pretubular aggregates (Yosipiv et al., 1997). The mentioned evidence suggests that BK is involved in renal embryonic development but little is known about its mechanism of action. Therefore, we propose the hypothesis that BK could participate in the cellular mechanisms that mediate the CD formation during the postnatal development of the kidney. Taking advantage that during the early postnatal period the embryonic structures are still present in the immature kidney, in the present study, we investigated the role of BK in the behavior of cultured CD cells isolated from renal papillae of neonatal rats. Our results showed that neonatal cultured cells form migratory colonies, favored by BK, and that BK, by its B2R, triggers the activation of the BK/B2R/PI3K/Akt pathway, which induces CD cell-cell association, colony compaction and development of ruffles and lamellipodia extension, typical structures of collective migratory colonies. These results lead us to suggest that these phenomena emulate the UB branching. Since UB branching is a requisite for correct renal development, our results can be considered as evidence that justifies the known physiological role of BK in renal development.

Materials and methods

Antibodies and reagents – We used the following primary antibodies: anti-B2 bradykinin receptor (mouse monoclonal IgG2b, Cat. #610451 1:100, BD Transduction Laboratories), anti-E-cadherin (rabbit polyclonal (H-108), Cat. #sc-7870 1:100, Santa Cruz Biotechnology), anti- β -catenin (mouse monoclonal IgG1, Cat. #C7082 1:100, Sigma-Aldrich), anti-phosphatidylinositol-4,5-bisphosphate and phosphatidylinositol-3,4,5-trisphosphate (PIP2 – mouse monoclonal IgM conjugated to biotin, Cat. #Z-B045 1:200. PIP3 - mouse monoclonal IgG, Cat. #Z-P345b 1:1000 - Echelon Biosciences),

anti-Rac1 (mouse monoclonal, Cat. #ARC03 1:100 Cytoskeleton, Inc), anti- Proliferating Cell Nuclear Antigen (PCNA) (mouse monoclonal IgG2a, Cat. # 555566 1:200 for immunocytochemistry, and 1:500 for western blot; BD Pharmingen), anti- Ret (rabbit polyclonal (H-300), Cat. #sc-13104 1:100, Santa Cruz Biotechnology), anti-phospho-p38 MAPK (Thr180/Tyr182), anti-Akt, and anti-phospho-Akt (Thr308) (Cat. #9215, #9272 and #9275, respectively; rabbit polyclonal antibodies, 1:100 both for immunocytochemistry and western blot - Cell Signaling Technology). Primary antibodies were detected using FITC- or TRITC-conjugated affinity purified goat anti-mouse or anti-rabbit antibodies (goat anti-mouse FITC: Cat. #115-096-072 1:200, goat anti-mouse TRITC Cat. #115-025-164 1:200, goat anti-rabbit FITC: Cat. #111-095-144 1:200, goat anti-rabbit TRITC Cat. #111-025-144 1:200 - Jackson ImmunoResearch). The lectin *Dolichos biflorus agglutinin* (DBA, biotinylated - Cat. #B-1035 1:250) was detected using TRITC-conjugated streptavidin (Cat. #016-020-084 1:400, Jackson ImmunoResearch). FITC-coupled phalloidin (Cat. #P5282 1:1250), bradykinin (Cat. #B3259), and HOE-140 (B2R antagonist - Cat. #H-157) were purchased from Sigma-Aldrich; LY294002 (PI3K inhibitor - Cat. #440202) from Calbiochem; Vectashield Mounting Medium (Cat. #H-1000) and DBA from Vector Laboratories; and the avidin-biotin-peroxidase kit (Cat. #K-0355) was purchased from Dako Ltd. All culture reagents were from Invitrogen, Thermo Scientific. All buffer solutions reagents were of analytical grade or higher, they were from Sigma-Aldrich or Merck, and were purchased from local commercial suppliers.

Animals and tissue preparation - All animals were handled according to the guidelines for Animal Care and Use of Laboratory Animals of the National University of La Rioja, La Rioja, Argentina (CICUAL-UNLaR). The animal protocol was reviewed and approved by the Ethics Committee for the CICUAL-UNLaR. Pregnant female Wistar rats of 70 day-old were used. After parturition, litter size was reduced to 8 pups / mother to ensure uniform nutrition. Five- to ten-day -old rats were used for the analyses. Adult male Wistar rats of 70 day-old (250-300 g) were also used. The newborn group consisted of 4 (immunofluorescence) to 7 (western blot) rat pups obtained from one

litter, using equal number of male and female rats per study group. In the adult group, 2 male rats from one litter were used for the B2R immunofluorescence study. The animals were housed in a light-controlled room with a 12:12 h light-dark cycle and allowed free access to water and standard rat chow. Animals were euthanized by decapitation, kidneys removed, and renal papillae isolated and collected on ice-cold 10 mM Tris-HCl, pH 7.4, containing 140 mM NaCl, 5 mM KCl, 2 mM MgSO₄, 1 mM CaCl₂ and 5.5 mM glucose.

Cell cultures, bradykinin and other treatments - In all experiments we applied a classical two-dimensional cell culture system, and the drugs were added manually with a micropipette. Primary cultures of CD cells were performed according to Stokes et al. (1987). Briefly, renal papillae were minced to 1-2 mm³ pieces and incubated at 37°C in sterile Tris buffer solution containing 0.1 % collagenase II under 95% O₂ / 5% CO₂. After 30-40 min, digestion was stopped and isolated cells and structures were separated by centrifugation at 28g for 2 min. The crude pellet containing most papillary cell types, tubular structures, and tissue debris was washed twice with phosphate buffered saline (PBS) and resuspended in Dulbecco's modified Eagle's medium (DMEM) with F-12 (1:1), 10 % fetal bovine serum (Natocor, Córdoba, Argentina), 100 U/ml penicillin and 100 µg/ml streptomycin. The enriched CD pellets were obtained by centrifugation at 28g for 2 min and resuspended in an adequate volume of DMEM/F-12. Enriched-tubular suspensions were seeded in sterile dry-glass coverslips placed in six-well multidishes. After growing at 37°C for 48 h, cultures were treated with 1 µM BK (final concentration) for 1-5 min. Incubations were stopped on ice and cells were rapidly processed for microscopy. When experiments were performed in the presence of the B2R antagonist HOE-140 (100 nM, final concentration), cells were preincubated for 30 min before BK stimulation, whereas when they were performed in the presence of LY294002 (10 µM, final concentration), cells were preincubated for 10 min before BK stimulation. To evaluate the B2R expression in primary cultured CD cells by immunocytochemistry, the cells were grown on six-well multidishes and samples were taken for 48 h, from the initial stage of culture (1 h after cell plating), every 4 h. To study the expression of PCNA and the phosphorylation of Akt and p-38

MAPK by immunoblot, primary cultured CD cells grown on six-well multidishes at 37°C for 48 h were treated with 1 μ M BK (5 min), in the presence or absence of 100 nM HOE-140 (30 min), or 10 μ M LY294002 (10 min). Incubations were stopped on ice and cells were rapidly scraped off with a rubber policeman and collected in PK lysis buffer (50 mM HEPES pH 7.5, 150 mM NaCl, 1.5 mM MgCl₂, 1 mM EGTA, 1 mM Na₃VO₄, 50 mM NaF, 1% Triton X-100, 10% glycerol, and a mixture of protease inhibitors (Sigma-Aldrich) (Cai et al., 2002). To ensure the complete disruption of the cells, suspensions were passed 10-20 times through a 29-gauge needle. Aliquots of total cell lysates were assayed for protein content by the method of Lowry (Lowry, 1951).

Immunocytochemistry - For immunostaining, cells treated as described above were fixed with methanol (at -20°C for 10 min) and acetone (at -20°C for 4 min), and blocked with 1% bovine serum albumin (BSA) in PBS. After fixation, cells were incubated with the appropriate combinations of antibodies and lectin- mentioned in *Antibodies and reagents* - overnight at 4°C in 1% BSA in PBS. Mouse and rabbit primary antibodies were detected using fluorescent FITC- or TRITC-conjugated goat anti-mouse or anti-rabbit antibodies. For lectin staining, cells were incubated with biotin-conjugated DBA dissolved in 1% BSA in PBS at a concentration of 25 μ g/ml. Positive cells were detected with TRITC-conjugated streptavidin. Nuclei were counterstained with Hoechst 33258. In cytoskeleton studies, cells were washed with PBS and fixed with 2 % paraformaldehyde solution in PBS for 20 min, permeabilized with a 0.1% Triton X-100 in PBS for 15 min, and blocked with 1% BSA in PBS. The cells were then washed with PBS and stained with FITC-coupled phalloidin. Finally, the cells were mounted using Vectashield Mounting Media and stored at 4°C until analysis. To study adherens junctions, the fixed cultured cells were stained with anti-E-cadherin and anti- β -catenin antibodies. Specimens were examined with a conventional fluorescence Olympus IX81 microscope with 20X LUCPlanFLN (0.45 NA air) or 40X UplanFLN (0.75 NA air) objectives. Images were acquired with an Olympus DP70 digital camera, with the acquisition software provided by the manufacturer. In experiments involving confocal microscopy, samples were examined with an Olympus FV300 Confocal Microscope (Model BX61), with the

Accepted Article

acquisition software FluoView version 3.3 provided by the manufacturer. Double fluorescence for green and red channels was visualized by using an argon-helium-neon laser. Double-stained confocal images were obtained by sequential scanning for each channel to eliminate the crosstalk of chromospheres. Optical sections obtained with an oil immersion 60X 1.4 NA objective were 0.5 μm . For xz assembled images and 3D reconstruction, the Image J version 1.51r software was used. All images were obtained with a cooled CCD camera and processed for output purposes using Adobe Photoshop software. When necessary, filters were applied to soften the images with the Image-Pro Plus Version 5.1.2 (Media Cybernetics, USA) module.

Immunoblot analysis - Total cell lysates (100 μg protein for Akt and p-Akt) were resolved by electrophoresis on a 10 % SDS-polyacrylamide gel under reducing conditions and transferred to polyvinylidene difluoride membranes. After blotting, membranes were treated with 5 % non-fat milk in Tris-buffered saline-Tween 20 (TBST) and incubated with the indicated antibodies. The primary interaction was evidenced by using the avidin-biotin-peroxidase and 3,3'-diaminobenzidine. For loading control, membranes were stained with Coomassie blue. The blots were scanned and signals quantified by optical densitometry with the Gel-Pro Analyzer 3.1.

Time-lapse assay – To perform time-lapse experiments, we used cultured 19 to 24-h-old CD cells. Cells were maintained on a heated platform (37°C) and imaged under differential interference contrast (DIC) on a Nikon Eclipse Ti microscope equipped with an oil immersion 60X, 1.40 NA (Plan Apo VC Nikon) objective, or imaged under phase contrast on an Olympus IX81 microscope equipped with an 40X PH LUCplanFLN (0.60 NA air) objective. A CD colony was randomly selected and images were captured every 20 seconds for 1 h 26 min using NIS-Element F 4.0 software and a digital Ds-Qi1Mc (Nikon) 1.3-megapixel camera, or with an Olympus DP70 digital camera, with the acquisition software provided by the manufacturer. BK (final concentration 1 μM) was added to the culture at 34 min 20 sec, and the behavior of the cultured CD cells was analyzed before and after BK stimulation. When experiments were performed in the presence of the B2R antagonist HOE-140 (100 nM), cells were preincubated for 30 min before BK stimulation, whereas

when they were performed in the presence of LY294002 (10 μ M), cells were preincubated for 20 min before BK stimulation. BK, as well as HOE-140 and LY294002, were added by a manual system (pipetting). After image acquisition, the movies were generated using the Image J version 1.51r software. These experiments were carried out in triplicate.

Image analysis – Cells were examined with a 40X UplanFLN (0.75 NA air) objective and the wide-field fluorescence microscopy images obtained were analyzed using Image-Pro Plus version 5.1.2 (Media Cybernetics). The total number of cells (nuclei), and the PCNA, Ret, PIP3- or Rac1-positive cells were counted for each condition: untreated cells (Control), treated cells with 1 μ M BK (1 min), in the presence or absence of 100 nM HOE-140 (30 min), or 10 μ M LY294002 (10 min). All positive signals in 30-180 cells for PCNA, 20-230 cells for Ret, 90-200 cells for PIP3 and 600-1000 cells for Rac-1 were randomly selected and analyzed for generation of quantitative data sets for each treatment, and three independent experiments were performed.

Pixel intensity profile from cell edge – Confocal images of Akt- and p-Akt-labeled cells were imported into Image-Pro Plus software. Cells were examined with an oil immersion 60X 1.4 NA objective, resulting in a pixel length of 0.23256 μ m after the spatial calibration was performed. The signal intensity was determined in 8 μ m to 30 μ m lines from the cell edge toward the cell center, for control and BK-treated cells respectively. Average intensity profiles were calculated from 10 regions per cell in 4–6 different cells per experimental condition (control and BK 5 min of stimulation), and three independent experiments were performed.

Quantification of the CD epithelial sheet area - To quantify the CD epithelial sheet area (in μ m²), DIC and phase contrast images from the time-lapse experiments were analysed using Image-Pro Plus version 5.1.2. Randomly selected CD cell colonies were analysed to generate quantitative data before and after BK, HOE-140, and LY294002 treatments. Cells were examined with an oil immersion 60X, 1.40 NA (Plan Apo VC Nikon) objective, resulting in a pixel length of 0.1537 μ m after performing the spatial calibration; or were examined with a 40X PH 0.60 NA (LUCplanFLN air) objective resulting in a pixel length of 0.3030 μ m. To calculate the area in μ m², the contour of

each colony in the DIC and phase contrast image (area of interest) was manually drawn by using the program mouse pointer. We established a valid range for the area measurement using the set range command of the software, specifying a minimum value of $0.25 \mu\text{m}^2$.

Statistical analysis - The statistical analysis was performed using GraphPad InStat version 3.01 program (GraphPad Software, Inc). Results were expressed as the mean \pm SEM. Data from control and different treatments were analyzed by unpaired *t*-test and unpaired *t*-test with Welch correction when standard deviations were considered not equal; and by ANOVA with “a posteriori” Tukey-Kramer multiple comparison test when differences were significant. Statistical significance was set at $p < 0.05$.

Results

BK induces CD cell association

CD cells from renal papillae of neonatal rats were isolated and primary cultures were performed and analyzed by staining with FITC-conjugated phalloidin. Primary cultured CD cells presented a high level of heterogeneity regarding the size of the colonies and the degree of cell association (Fig. 1A,B). When cells were not yet associated, $1 \mu\text{M}$ BK was added. The low-magnification pictures in Fig. 1 show the overall effect of the different treatments in cultured CD cells. After 48 h, cultured cells formed colonies with loosely associated cells with few areas of cell-cell contact (Fig. 1C). In the magnified image, it is possible to visualize cells with extending filopodia, which made contact with opposite filopodia of neighboring cells (Fig. 1D, arrows), and a prominent actin-rich cell cortex drawing individual cells. After 1 minute of BK stimulation, the 48 h-cultured cells became more tightly associated (Fig. 1E,F). Phalloidin-stained bundles of actin surrounding individual cells appeared attenuated, while bundles of actin were observed along the periphery of the cell colony, denoting that BK induced cell compaction (Fig. 1E, arrows). We further analyzed the effect of BK on colonies of CD cells with higher level of cell association. Under this condition, the untreated

cells exhibited a well-delineated colony (Fig. 1G). After BK treatment, the formation of a strong continuous actin belt surrounding the colonies, accompanied by a notorious polarization of the semicircular actin bundle in the periphery of the colony, was evident (Fig. 1H). Consistent with the typical phenotype of a collective migratory epithelial sheet, a group of cells extending lamellipodial protrusions evoked colony polarization, which seemed to be indicating the direction of the migration (Fig. 1H, arrows). By contrast, it was not possible to define a leading and a rear edge in untreated colonies in which cells exhibited lamellipodia with no specific localization (Fig. 1G, arrows).

Time-lapse experiments recording the behavior of the cultured CD cells before and after BK stimulation showed that a group of CD cells behaved as a collective migratory unit, exhibiting an important protrusive activity. At any given time, many marginal cells were extending lamellipodia in all directions. During the recording, the cells remained closely attached, without losing their contacts with other cells (Fig. 2A, see also Movie 1). After adding BK, a prominent increase was observed in the rate of lamellipodia and membrane ruffle extension of marginal cells (Fig. 2A,B, arrows, see also Movies 1 and 2). Also, after BK stimulation, some cells appeared to physically embed their plasma membrane into the adjacent cell membrane. Thereafter, a continuous line was formed, denoting more mature cell-cell adhesion (Fig. 2C, arrow, see also Movie 3). To confirm the BK-induced compaction of the colony, the area of the colonies was quantitatively analyzed before and after BK treatment. The total area of epithelial sheets decreased by 10% (Fig. 2D). This decrease was significant because there was no change in the cell number or individual cell area.

Taken together, these results suggest that BK induced and maintained cell-cell association without any discontinuity in the monolayer, thus favoring the acquisition of the collective migratory phenotype of CD cells.

BK-induced CD cell association is mediated by B2R activation

To determine whether BK effects were triggered by B2R activation, we preincubated cultured cells for 30 min in the presence of the B2R antagonist HOE-140 (100 nM, final concentration) before BK stimulation. As control, the cultured cells were incubated during 30 min in the presence of HOE-140 alone (HOE-Control). In both control and cells pretreated with the B2R antagonist, loosely associated cells with extending filopodia were observed (Fig. 3A-C). In contrast to that observed in cells treated only with BK (Fig. 3D), after the pretreatment with HOE-140, the BK-induced cell-cell adhesion was partially prevented (Fig. 3E), the number of filopodia between cells was decreased, and the F-actin cortex in individual cells became more evident, as denoted by phalloidin staining (Fig. 3F), resulting in a diminished level of compaction.

The time-lapse recording using phase-contrast optical microscopy showed that, in the presence of the B2R antagonist, the membrane ruffling process was absent (Fig. 4A,C see also Movie 4), and although the cells remained associated inside the colony, the BK-induced cell compaction was completely prevented, as denoted by the quantitative analysis of the area (HOE-C vs HOE-BK, non-significant p value).

These results suggest that BK-induced cell aggregation and formation of a colony with a collective migratory phenotype depend on B2R stimulation.

The PI3K/Akt signaling pathway is involved in BK-induced CD cell association

It is accepted that, among others, the PI3K/Akt signaling pathway is implicated in various physiological mechanisms related to cell adhesion and motility (Cantley, 2002, Kölsch et al., 2008). Thus, we next investigated whether the inhibition of PI3K activity modify BK effects on cultured CD cells. The pretreatment with the PI3K inhibitor LY294002 impaired the BK-induced cell-cell adhesion. It is worth noting that the actin belt surrounding the colonies was not formed and that the number of filopodia between cells decreased (Fig. 3H, insert, and 3I). Time-lapse experiments

showed that, after the pretreatment with the PI3K inhibitor, the lamellipodial extension was greatly suppressed (Fig. 4B, see also Movie 5), and the addition of BK did not affect the rate or length of these cytoskeletal protrusions. The quantitative image analysis of the area demonstrated that BK-induced cell compaction was suppressed by LY294002 (LY-C vs LY-BK, non-significant p value) (Fig. 4C). These data strongly suggest that PI3K activity is involved in BK-induced cell-cell association and formation of collective migratory structures.

It is known that, upon activation, PI3K translocates to the plasma membrane, where it converts phosphatidylinositol-4,5-bisphosphate (PIP2) to phosphatidylinositol-3,4,5-trisphosphate (PIP3). Through the use of specific antibodies, we analyzed the distribution of both polyphosphoinositides in cultured CD cells after BK stimulation, in the presence or absence of the B2R antagonist. Under basal conditions, two subpopulations of cells were distinguished in the same colony: one formed by PIP3-negative/PIP2-positive cells, larger than the other formed by PIP3-positive/PIP2-positive cells (Fig. 5A,B). The number of CD cells containing PIP3 significantly increased after BK stimulation (C vs BK, $p=0.02$) (Fig. 5A-D, and quantitative analysis), but when the cells were pretreated with the B2R antagonist (Fig. 5E,H), the increase in PIP3-positive cells appeared attenuated (HOE-C vs HOE-BK, non-significant p value) (Fig. 5E-H, and quantitative analysis).

It is known that PIP3 recruits the serine/threonine kinase Akt, leading to its phosphorylation and activation, thus, acting as a critical signal downstream PI3K activation. The immunoblot analysis of primary cultured cell lysates revealed that BK caused an increase in the amount of phosphorylated Akt (Thr308), not observed when CD cells were pretreated with the B2R antagonist HOE-140 or the PI3K inhibitor (Fig. 6). Then, we analyzed the distribution of Akt and p-Akt (Thr308) in CD cells by immunofluorescence staining and found low fluorescence intensity of the p-Akt signal in untreated CD cells (Fig. 7A). After stimulation with BK, the intensity of the p-Akt signal increased and was mainly located in the membrane of some cells of the edge of the colony (Fig. 7B, arrows). In contrast, the unphosphorylated form of Akt was similarly and uniformly distributed in the cytosol in both control and BK-treated CD cells (Fig. 7C,D). The distribution of these signals in the whole

Accepted Article

cell body was then carefully examined by studying the pixel intensity profile of the fluorescence of Akt and p-Akt from the cell edge toward the nucleus. p-Akt was mainly accumulated in the perinuclear region and in the cell periphery. Analysis of the pixel intensity profile of untreated cells showed a diffuse localization of Akt in the cytosol, before and after 5 min of BK stimulation (Fig. 7E). By contrast, after 5 min of BK stimulation, p-Akt was mainly accumulated in the cell periphery and in the perinuclear region, while in the untreated cells the p-Akt signal was lower and presented a more diffuse pattern of distribution throughout the cytosol (Fig. 7F). Taken together, these results suggest that, in immature CD cells, after binding to its B2R, BK activates the PI3K signaling pathway, which involves downstream Akt activation.

Yosipiv et al. reported that BK-B2R is involved in the regulation of DNA synthesis and cell proliferation in neonatal rat kidney (Yosipiv et al., 1997). Considering that, the Proliferating Cell Nuclear Antigen (PCNA) is an essential marker for cellular DNA synthesis and it is expressed at high levels in the S phase of the cell cycle (Leonardi et al., 1992), we further explored the expression of PCNA in response to BK in cultured CD cells. The quantitative analysis of the immunofluorescence images showed that exposure of CD cells to BK during 1 and 5 min (1 min, not shown) causes a significant increase in the number of PCNA-positive cells, with a fluorescence signal accumulated in the nucleus (C vs BK, $p=0.0001$) (Fig. 8A-D, and quantitative analysis). Consistently, the immunoblot analysis revealed a significant increase in the total amount of PCNA after 5 min of BK stimulation (C vs BK, $p= 0.0005$), not observed when CD cells were pretreated with the PI3K inhibitor, LY294002 (LY-C vs LY-BK, $p= 0.0001$) (Fig. 8E). In addition, Tang et al. have demonstrated that p38 MAPK pathway is implicated in the branching morphogenesis of the UB epithelium at latter developmental stages (Tang et al, 2002). To determine whether p38 MAPK is activated in response to BK in immature CD cells, we assessed the phosphorylated (activated) state of p38 MAPK in cultured cells. The immunoblot analysis revealed a significant increase in the amount of the activated form of p38 MAPK (C vs BK, $p= 0.004$) (Fig. 8F). By contrast, the

pretreatment with LY294002 impaired the BK-induced phospho-p38 MAPK increase, suggesting that PI3K activity is involved in BK-induced p38 MAPK activation (LY-C vs LY-BK, $p=0.0001$) (Fig. 8F).

In addition to Akt, Rac has also been indicated as a key downstream effector of PI3K (Kölsch et al., 2008). Since it is known that Rac is involved in the formation of lamellipodia and membrane ruffles to facilitate cell motility (Ridley et al., 1992) and considering that BK induces these processes (Fig. 2, Movies 1 and 2), we next analyzed the protein expression and distribution of Rac1 in CD cells by immunofluorescence. For this purpose, we used a specific antibody that recognizes the Rac1 isoform, which does not cross-react with other members of the Rho GTPase family or other Rac isoforms. In control CD cells, the fluorescent signal of Rac1 was weakly positive only in some cells (Fig. 9A-C). After stimulation with BK, the number of cells expressing the protein significantly increased (C vs BK, $p=0.01$) (Fig. 9D-F, and quantitative analysis). Interestingly, these cells were not located at random, but rather occupied a particular area of the colony (Fig. 9E). When CD cells were pretreated with the specific antagonist of B2R, HOE-140, the increase in Rac1-positive CD cells appeared attenuated (HOE-C vs HOE-BK, non-significant p value) (Fig. 9G-L, and quantitative analysis) and were located at random. When cells were incubated with the PI3K inhibitor, LY294002, prior to BK stimulation, the number of Rac1-positive cells was very low, and were not part of the CD cell sheet (LY-C vs LY-BK, non-significant p value) (Fig. 9M-R, and quantitative analysis). Taken together, these results suggest that, after binding to its B2R, BK induces Rac1 expression in immature CD cells.

In the embryonic kidney, Ret is an essential component of the signaling pathway which regulates UB outgrowth and branching morphogenesis through the PI3K pathway (Tang et al. 2002; Wenting and Nelson, 2012), and also coordinates the proliferation and migration of UB cells (Dressler, 2006, 2009; Kim and Dressler, 2007; Pohl et al. 2000; Tang et al., 2002). In order to evaluate whether BK has any effect on the expression of Ret, we simultaneously analyzed the protein expression and

lectin *Dolichos biflorus agglutinin* (DBA) binding as a marker of CD cells by immunofluorescence. Besides being a general marker of the developing CD, DBA is also used as a sensitive and reverse indicator of morphogenic activity related to branching morphogenesis (Michael et al., 2007). On the other hand, it has been reported that the lack of DBA-positive signal in the developing CD corresponds to zones of enhanced cell proliferation (Michael et al., 2007). Under basal conditions, the Ret fluorescent signal was weak and presented a diffuse pattern of distribution throughout the cytosol of a low number of cells, mainly in those not stained with DBA lectin (Fig. 10A-C). After BK stimulation, the number of CD cells expressing the protein significantly increased (C vs BK 1 min, and C vs BK 5 min, $p=0.001$; BK 1 min vs BK 5 min, non-significant p value), and the fluorescent signal was mainly observed in the nucleus (Fig. 10D-I, and quantitative analysis). The results indicate that BK induces Ret expression and its mobilization to the nucleus in cultured CD cells. The BK-induced nuclear accumulation of Ret suggests that it is operating as a transcription factor in neonatal CD cells.

BK is involved in early adhesive events between immature CD cells

Taking into account that the CD cell-cell association induced by BK stimulation was impaired when cells were pretreated with a B2R antagonist (Fig. 3E), we next examined the evolution of B2R expression for 48 h, from the initial stage of culture (1 h after cell plating), taking samples every 4 h. We also examined lectin DBA binding as a marker of CD cells. The evaluation of CD cells reacting with DBA revealed that, after 48 h of culture, there were two major populations of cells in the same colony: one formed by DBA strongly positive cells with typical epithelial morphology, and the other formed by negatively or weakly DBA-positive cells (Fig. 11A). To study the origin of these two cell populations, we analyzed B2R expression from 1 h after plating, taking samples every 4 h. CD cells from early cultures looked dispersed, some were DBA-positive but most of them expressed B2R (Fig. 11D-F). From 4 to 48 h of culture, faint or no B2R immunoreactivity was observed in the cells displaying a strong positive reaction with DBA (Fig. 11G-L). Interestingly,

cells expressing B2R exhibited either no or weakly positive DBA staining (Fig. 11C,I,L, arrows). We noted that the longer the culture period, the lower the expression of the receptor. Besides, most of the primary cultured CD cells isolated from renal papillae of adult rats were positively stained with the lectin and only a few of them were B2R-positive, showing a punctuate pattern in the perinuclear zone and thus differing from the cytosolic B2R immunostaining observed in neonatal CD cells (Fig. 11M-O, arrows).

These results suggest that the expression of B2R was inversely related to the intensity of DBA staining, and so, to the degree of CD cell maturation.

Cultured CD cells conserved the property to attach with their self-formed extracellular matrix and also generated adhesive cell-cell contacts, thus mimicking their behavior in intact tissue. The first step in cell-cell adhesion is the establishment of adherens junctions (AJ) by homophilic cadherin interactions of adjacent cells (Cavey et al., 2008). Initially, the AJ complex is immature and unstable, but as cells undergo differentiation, the AJ complex matures and becomes more stable. In this process, the E-cadherin-mediated formation of the AJ complex is critical for the maintenance of the epithelial tissue architecture (Knust and Bossinger, 2002; Nelson, 2003; Guillot and Lecuit, 2013). To analyze the evolution of CD organization, we evaluated the expression of B2R and DBA staining together with E-cadherin expression. We observed that groups of CD cells with different degree of maturation coexisted in the same colony, denoting the presence of a high level of heterogeneity with regards to the cell-cell association. The most mature cells, which were positive for DBA staining, exhibited E-cadherin delimiting their borders (Fig. 12A-C, arrows). It is worth noting that as CD cells with more mature AJ lost B2R expression, B2R-positive cells remained mainly located as the outermost limit cells of the colony (Fig. 12D-F, arrows). Analysis of the 3D assembled confocal sections and xz sections of the cells showed more clearly that cells containing E-cadherin in their borders did not express the receptor and that B2R-positive cells were part of the colony (Fig. 12G, G' and xz reconstruction). Therefore, the lack of B2R immunostaining in cells that had established cell-cell junctions suggests that BK/B2R is only involved in early adhesive

Accepted Article

events of CD organization. We also observed that when cultured CD cells were treated with BK, E-cadherin delimited the lateral membrane at cell-cell contacts of a higher number of cells compared with untreated cells, thereby reflecting the presence of AJ, better observed in the magnifications shown as inserts (Fig. 13A,C,E, inserts). When cells were pretreated with the B2R antagonist HOE-140 prior to the addition of BK, no E-cadherin cell-cell contacts were observed (Fig. 13B,D,F).

β -catenin is an adaptor protein that stabilizes E-cadherin-mediated cell-cell adhesion. Since β -catenin is associated with the cytosolic domain of E-cadherin to form the adherent complex, we also analyzed β -catenin expression and distribution in BK-stimulated CD cells, in the presence and absence of the B2R antagonist. Figure 14A shows part of a colony showing an intermediate degree of compaction. Under these conditions, some cells exhibited filopodia immunostained with β -catenin, which denotes their affinity to associate (Fig. 14C, arrows), whereas, in cells with a higher degree of association, β -catenin was distributed delimiting their borders (Fig. 14A, cell group on the left). After the addition of BK, the degree of cell compaction was increased, the edge of the colonies became more regular, and the β -catenin immunostaining was continuously located in the cell borders (Fig. 14B,D). By contrast, when the cells were treated with the B2R antagonist, the colonies showed a lower degree of compaction, and the β -catenin signal was not regularly and continuously distributed at the cell borders (Fig. 14F), as shown in BK-stimulated CD cells in the absence of the antagonist (Fig. 14B,D). These data reinforce the notion that BK induces and maintains cell-cell association to assure correct CD formation.

Discussion

In rats, the kidney is not fully developed at birth (Dodge, 1997; Kahane et al., 1995; Márquez et al., 2002). We have previously reported that, until postnatal day 10, most renal papillary cells are found in different phases of the cell cycle, many of them have an embryonic phenotype (Kahane et al., 1995; Márquez et al., 2002), and blind ends of CD branches underneath the capsule are still present

(Márquez et al., 2002). Thus, we concluded that the renal papilla of the neonate rat contains immature collecting tubules in process of maturation.

In the present work, we isolated CD cells from renal papillae of five- to ten-day-old rats and performed primary cultures. Cells preserved their ability to attach with their self-formed extracellular matrix and to join to each other. *In vivo* changes during renal development are very fast. In primary cultures, these changes are reflected by the high level of heterogeneity related to the degree of CD cell association and epithelial sheet maturation at different times of culture. Consequently, the coexistence of colonies of recent formation and others in a more advanced state of maturation can be observed.

It has been reported that the expression and activity of angiotensin converting enzyme I (kininase II), the main kinin-degrading enzyme, are low in the fetal and neonatal rat kidney, thus allowing intrarenal BK accumulation during the developing stage (Yosipiv et al., 1994). *In vivo* treatment of newborn rats with a selective BK-B2R antagonist results in impaired kidney growth, but has no effect on the adult kidney (Yosipiv et al., 1997). Under normal conditions, B2R knockout mice are viable, normotensive, and do not develop structural renal abnormality (Alfie et al., 1997; El-Dahr et al., 2000b), probably due to the fact that, as Duka and collaborators have demonstrated in B2R-null mice, the gene disruption induced B1R up-regulation (Duka et al., 2001, 2008). However, B2R null mice acquires an aberrant kidney phenotype and die shortly after birth when they are submitted to embryonic stress conditions (El-Dahr et al., 2000b). Likewise, rats in gestation pretreated with a selective B2R antagonist and then submitted to a high salt concentration intake showed an aberrant segmental nephrogenesis affecting the distal nephron, which is the main site of the kininogen and B2R expression during early renal development (El-Dahr et al., 2000a). B1R gene expression is low during fetal life, and is up-regulated postnatally (Bulut et al., 2009) and contrary to what happens with B2R, B1R is not expressed in the collecting duct, being almost exclusively expressed in the proximal tubules (Bulut et al., 2009). While BK preferentially stimulates the B2R, Des-Arg9-BK- a

natural metabolite of BK produced by the carboxypeptidase kinase I- stimulates the B1 receptor. B1R knockout mice are viable although exhibiting inflammatory dysfunctions (Pesquero et al. 2000). A formal evaluation of nephrogenesis in this model has not been reported. These evidences support a role for BK during kidney development, but its functional relevance is still not entirely understood. Therefore, we investigated the role of BK in the behavior of CD cells in primary culture.

Branching morphogenesis is a form of collective cell migration, where cells remain connected as they move (Friedl, 2004; Weijer, 2009; Scarpa and Mayor, 2016), and the leading edge is formed by one or several cells that develop actin-mediated ruffles (Hegerfeldt, 2002). Consistently, our present results indicate that BK promoted a high increase in the rate of lamellipodia and membrane ruffle extension and the acquisition of a higher level of cell compaction, thus emulating the process of branching morphogenesis. The pretreatment with the B2R antagonist HOE-140 impaired BK-induced cell-cell adhesion and membrane ruffle formation, indicating that the effects of BK depend on B2R stimulation. In colonies with a higher level of cell association, BK induced a notorious polarization of the semicircular actin bundle in the periphery of the colony, where a group of cells containing lamellipodia indicated the direction of the migration, thus displaying a typical phenotype of a collective migratory epithelial sheet. By contrast, no leading and a rear edge of the colonies were observed in untreated cells. Taken together, our results suggest that BK-B2R interaction is implicated in the stabilization of migratory cell colonies.

During embryonic renal development, B2R gene expression is highly activated and localized in the ramifications of the developing CD (El-Dahr, 1997, 2000a, 2004). As we show in the present report, B2R appeared highly expressed in recently cultured CD cells as well as in newly formed colonies. As the culture time increased, B2R expression decreased and the DBA-positive signal increased until no B2R immunoreactivity was observed in CD cells displaying a strong positive reaction for DBA. By contrast, primary cultured CD cells derived from adult kidney were highly positive for DBA and exhibited almost no B2R immunostaining. Thus, we suggest that the DBA-positive cells

represent the tubular epithelial subpopulation with a higher degree of differentiation. This concept can be further supported by the results obtained using E-cadherin, where cells that showed positive E-cadherin signal in AJ were also highly positive for DBA but devoid of B2R signal. The lack of B2R immunostaining in cells that had already established cell-cell junctions, and therefore had a higher degree of maturation, suggests that BK is mostly involved only in early adhesive events.

The signaling pathways that affect branching morphogenesis in the kidney have been widely investigated (Pohl et al., 2000). PI3K has been shown to be essential for the initial outgrowth and branching morphogenesis in mice and an altered signaling through this pathway contributes to renal cyst formation (Tang et al., 2002; Pozzi et al., 2006; Wenting and Nelson, 2012). Our results indicate that PI3K is in fact involved in BK-induced CD cell-cell association and the acquisition of collective migration phenotype since, when the kinase was pharmacologically inhibited, the number of membrane ruffles and filopodia between cells, structures involved in migration and cell-cell interaction respectively, were diminished. Several studies have pointed out that the activation of PI3K and its target, Akt, in response to glial cell line-derived neurotrophic factor (GDNF)-mediated Ret activation regulate UB outgrowth and branching morphogenesis (Doyeob and Dressler, 2007, Tang et al., 2002). Our results show that, in cultured CD cells isolated from renal papillae of neonatal rats, the activation of PI3K mediated by BK-binding to its B2R induces Akt activation, which occurs only in the absence of the B2R antagonist and of the PI3K inhibitor. Our results indicate that, in cultured CD cells isolated from renal papillae of neonatal rats, Akt kinase, acting downstream PI3K, would participate in the generation of BK-induced phenomena already described.

In the present work, we provide experimental evidences linking BK stimulation with DNA synthesis by a mechanism involving PI3K activation. On the other hand, we also show that BK by PI3K activation stimulates p38 MAPK pathway. Due to the known effect of p38 pathway in branching morphogenesis (Tang et al, 2002), we can speculate that activation of PI3K/AKT

pathway by BK can also participate in the modulation of branching morphogenesis in neonatal CD cells.

In addition to Akt, Rac protein can also be activated as a downstream effector of PI3K (Kölsch et al., 2008). Since Rac is known to be involved in the formation of lamellipodia (Etienne-Manneville and Hall, 2002; Ridley et al., 1992; Kölsch et al., 2008) and cell adhesion structures (Sugihara et al., 1998; Yap and Kovacs, 2003) and we have shown that BK is involved in the induction of these processes, we also investigated Rac expression. Of the three isoforms described, only the Rac1 isoform was studied since it is the only one that is expressed in all cell types (Didsbury et al., 1989; Haataja et al., 1997). It has been reported that during cell migration, Rac1, through Arp2/3, mediates the assembly of actin branching filaments at the leading edge (Ridley et al., 1992, 2003). Our results show that BK treatment induces an increase in Rac1 expression in CD cells, which show a polarized distribution in the colony. Recent works have shown that Rac is first activated in some epithelial cells of the free borders during the collective cell migration, which leads to Rac activation in the rest of the cells as well as to the formation of lamellipodia in free border cells and small cryptic lamellipodia in cells located in the center of the epithelial sheet (Lebreton and Casanova, 2014; Scarpa and Mayor, 2016). Therefore, the polarized distribution of CD cells expressing Rac1 within the colony following BK stimulation seems to correlate to the distribution of the active Rac form in epithelial cell sheets, described by the aforementioned authors. Together, PI3K/Akt and PI3K/Rac1 would constitute key signaling pathways in the mechanisms of action of BK, by its B2R, in the developing CD by favoring the collective migration during renal development. Figure 15 shows an outline of the results discussed up to this point.

During nephrogenesis, to favor the migration of developing CD epithelial cells, a delicate balance between proliferation, cell motility and maintenance of cell-cell adhesions must be preserved. Our present results strongly suggest that BK is an important factor in this process. The migration of cells requires actin cytoskeleton rearrangements and the formation of lamellipodia and ruffles, as

observed upon BK stimulation in cultured CD cells. It is accepted that the GDNF/Ret signaling pathway regulates UB outgrowth and coordinates the proliferation and migration of UB cells, thus maintaining the integrity of the bud as an epithelial structure (Dressler, 2006, 2009; Kim and Dressler, 2007; Pohl et al. 2000; Tang et al., 2002). However, it has been reported that the Ret pathway is not the only promoter of these processes, as a significant proportion of Ret mutant kidneys still exhibit a rudimentary bud (Schuchardt et al, 1996). In the embryonic kidney, Ret expression becomes restricted to the growing tips of the bud, as branching morphogenesis progresses (Pachnis et al, 1993), and several studies have shown that UB tip cells, unlike stalk cells, do not bind DBA lectin (Michael et al., 2007; Sweeney et al., 2008). Although in our primary cultures of CD cells we can not distinguish tip from stalk cells, we observed a reduced or absence of Ret expression in DBA lectin stained cultured CD cells, which share similar lectin-binding characteristics of UB tip cells. On the other hand, it has been reported that the lack of DBA-positive signal in the developing CD corresponds to zones of enhanced cell proliferation (Michael et al., 2007). Our results indicate that BK has a stimulatory effect on Ret expression in DBA-negative CD cells, and also induces a nuclear location of the protein probably to operate as a transcription factor to induce cell proliferation,

Taken together, our results suggest that BK exerts a myriad of positive effects, all contributing to the development of the postnatal kidney. On the basis of our results, and considering that the expression of B2R appears very early during development, we propose that BK is one of those promoter factors. For this reason, we suggest that the signaling pathways initiated by GDNF and BK would probably act in a complementary manner. It has been described that the pharmacological blockade of B2R during the fetal stage causes hypoplasia and abnormal differentiation of the rat renal tubules, and delays renal growth during postnatal development (El-Dahr et al., 1997; Yosipiv et al., 1997). Therefore, if both routes were redundant, and not complementary, one route would

replace the other, and by inhibiting either of them, renal development would normally occur, something that does not happen.

Considering that the penetration of the UB in the metanephric mesenchyme is the physiological strategy to finally organize the entire kidney, the fact that BK/B2R plays a role in the initial formation and maintenance of the UB-derived CD allows us to suggest that BK/B2R constitutes at least an additional important pathway for kidney development.

In conclusion, the present study, performed with CD cells that were not genetically manipulated, provides new experimental evidence supporting a novel role of BK during renal postnatal development. We propose that BK, acting through B2R, favors cell compaction and increases CD collective cell motility. Our results indicate that the actions of BK mediated upon PI3K activation were also due to the downstream Akt and Rac1 pathways. We interpret that such behavior facilitates the collective advance of the UB and developing CD from the papilla to the renal cortex during nephrogenesis, where the mutual induction between the metanephric mesenchyme and the UB takes place, giving rise to the nephron and to the CD system, respectively. Since B2R blockade results in abnormal tubular differentiation (Yosipiv et al., 1994; Yosipiv et al., 1997), understanding the physiological mechanisms that underlie the behavior of UB and derived CD cells is crucial to gain insights into the etiology of human congenital renal malformation and kidney diseases.

Acknowledgments – Mr. Roberto Fernández, for the technical assistance in confocal microscopy.

References

- Alfie ME, Sigmon DH, Pomposiello SI, Carretero OA. 1997. Effect of high salt intake in mutant mice lacking bradykinin-B2 receptors. *Hypertension* 29: 483-487.
- Alhenc-Gelas F, Marchetti J, Allegrini J, Corvol P and Menard J. 1981. Measurement of urinary kallikrein activity species differences in kinin production. *BiochimBiophysActa*677: 477-488.
- Aperia A, Celsi G. 1992. Ontogenic processes in nephron epithelia. Structure, enzymes, and function. In: Seldin DW, Giebisch G, editors. *The kidney: physiology and pathology*. New York: Raven Press. p 803-828.
- Bulut OP, Dipp S, El-Dahr S. 2009. Ontogeny of bradykinin B1 receptors in the mouse kidney. *Pediatr Res* 665: 519-523.
- Cai Y, Lechner MS, Nihalani D, Prindle MJ, Holzman LB, Dressler GR. 2002. Phosphorylation of Pax2 by the c-Jun N-terminal kinase and enhanced Pax2-dependent transcription activation. *J BiolChem* 277:1217–1222.
- Cantley LC. 2002. The phosphoinositide 3-kinase pathway. *Science* 296:1655-1657.
- Cavey M, Rauzi M, Lenne PF, Lecuit T. 2008. A two-tiered mechanism for stabilization and immobilization of E-cadherin. *Nature* 453:751–756.
- Didsbury J, Weber RF, Bokoch GM, Evans T, Snyderman R. 1989. rac, a novel ras-related family of proteins that are botulinum toxin substrates. *J BiolChem* 264:16378-16382.
- Dodge AH. 1997. Introduction: review of microscopic studies on the fetal and neonatal kidney. *Microsc Res Tech* 39:205-210.
- Doyeob K, Dressler GR. 2007. PTEN modulates GDNF/RET-mediated chemotaxis and branching morphogenesis in the developing kidney. *DevBiol* 307:290-299.
- Dressler GR. 2006. The Cellular Basis of Kidney Development. *Annu Rev Cell DevBiol* 22: 509–529.

- Dressler GR. 2009. Advances in early kidney specification, development, and patterning. *Development* 136:3863-3874.
- Duka I, Kintsurashvili E, Gavras I, Johns C, Bresnahan M, Gavras H. 2001 Vasoactive potential of the B(1) bradykinin receptor in normotension and hypertension. *Circ Res* 88:275–281.
- Duka A, Kintsurashvili E, Duka I, Ona D, Hopkins TA, Bader M, Gavras I, Gavras H. 2008. Angiotensin-converting enzyme inhibition after experimental myocardial infarct: role of the kinin B1 and B2 receptors. *Hypertension* 51:1352–1357.
- El-Dahr SS and Chao J. 1992. Spatial and temporal expression of kallikrein and its mRNA during nephron maturation. *Am J Physiol* 262:F705-711.
- El-Dahr SS, Figueroa CD, Gonzalez CB, Muller-Esterl W. 1997. Ontogeny of bradykinin B2 receptors in the rat kidney: Implications for segmental nephron maturation. *Kidney Int* 51:739-749.
- El-Dahr SS, Dipp S, Yosipiv IV, Carbine LA. 1998. Activation of kininogen expression during distal nephron differentiation. *Am J Physiol* 44:F173-182.
- El-Dahr SS, Dipp S, Meleg-Smith S, Pinna-Parpaglia P, Madeddu P. 2000a. Fetal ontogeny and role of metanephric bradykinin B2 receptors. *Pediatr Nephrol* 14:288-296.
- El-Dahr SS, Harrison-Bernard LM, Dipp S, Yosipiv IV, Meleg-Smith S. 2000b. Bradykinin B2 null mice are prone to renal dysplasia: gene-environment interactions in kidney development. *Physiol Genomics* 3:121-131.
- El-Dahr SS. 2004. Spatial expression of the Kallikrein-Kinin system during nephrogenesis. *Histol Histopathol* 19:1301-1310.
- Etienne-Manneville S, Hall A. 2002. Rho GTPases in cell biology. *Nature* 420:629-635.
- Friedl P. 2004. Prespecification and plasticity: shifting mechanisms of cell migration. *Curr Opin Cell Biol* 16:14-23.

- Guillot C, Lecuit T. 2013. Mechanics of epithelial tissue homeostasis and morphogenesis. *Science* 340:1185-1189.
- Haataja L, Groffen J, Heisterkamp N. 1997. Characterization of RAC3, a novel member of the Rho family. *J BiolChem* 272:20384-20388.
- Hagiwara Y, Kojima M, Hayashi I, Oh-Ishi S. 1995. Demonstration of derivation of rat urinary bradykinin from plasma low-molecular-weight kininogen: a study using kininogen-deficient rats. *BiochemBiophys Res Com* 204:1219-1224.
- Hegerfeldt Y, Tusch M, Brocker EB, Friedl P. 2002. Collective cell movement in primary melanoma explants: plasticity of cell-cell interaction, β 1-integrin function, and migration strategies. *Cancer Res* 62:2125-2130.
- Hilgenfeldt U, StanekCh, Lukasova M, Schnolzer M, Lewicka M. 2005. Rat tissue kallikrein releases a kallidin-like peptide from rat low-molecular-weight kininogen. *British J Pharmacol* 146:958–963.
- Kahane VL, Cutrin JC, Setton CP, Fernandez MC, Catz SD, Sterin-Speziale NB. 1995. Biochemical and morphological changes in the developing kidney. *Biol Neonate* 68:141-152.
- Kato H, Enjyoji K, Miyata T, Hayashi I, Oh-ishi S, Iwanaga S. 1985. Demonstration of arginyl-bradykinin moiety in rat HMW kininogen: direct evidence for liberation of bradykinin by rat glandular kallikreins. *BiochemBiophys Res Com* 227:289-225.
- Kim D, Dressler GR. 2007. PTEN modulates GDNF/RET-mediated chemotaxis and branching morphogenesis in the developing kidney. *DevBiol* 307:290-299.
- Kitamura N, Takagaki Y, Furuto S, Tanaka T, Nawa H, Nakanishi S. 1983. A single gene for bovine high molecular weight and low molecular weight kininogens. *Nature* 305:545-549.
- Knust E, Bossinger O. 2002. Composition and formation of intercellular junctions in epithelial cells. *Science* 298:1955–1959.

- Kölsch V, Charest PG, Firtel RA. 2008. The regulation of cell motility and chemotaxis by phospholipid signaling. *J Cell Sci* 121:551–559.
- Lebreton G, Casanova J. 2014. Specification of leading and trailing cell features during collective migration in the *Drosophila* trachea. *J Cell Sci* 127:465–474.
- Leonardi E, Girlando S, Serio G, Mauri FA, Perrone G, Scampini S, Dalla PP, Barbareschi M. 1992. PCNA and Ki67 expression in breast carcinoma: Correlations with clinical and biological variables. *J ClinPathol* 45:416–419.
- Lowry OH, et al. 1951. Protein measurement with the Folin phenol reagent. *J BiolChem* 193(1):265-75.
- Márquez MG, Cabrera I, Serrano DJ, Sterin-Speziale NB. 2002. Cell proliferation and morphometric changes in the rat kidney during postnatal development. *AnatEmbriol* 205:431-440.
- Michael L, Sweeney DE, Davies JA. 2007. The lectin *Dolichos biflorus* agglutinin is a sensitive indicator of branching morphogenetic activity in the developing mouse metanephric collecting duct system. *J Anat* 210:89–97.
- Nelson WJ. 2003. Epithelial cell polarity from the outside looping in. *Physiology (Bethesda)* 18:143–146.
- Pachnis V, Mankoo BS, Costantini F. 1993. Expression of the *c-ret* proto-oncogene during mouse embryogenesis. *Development* 119:1005–1017.
- Pesquero JB, Araujo RC, Heppenstall PA, Stucky CL, Silva JA Jr, Walther T, Oliveira SM, Pesquero JL, Paiva AC, Calixto JB, Lewin GR, Bader M. 2000. Hypoalgesia and altered inflammatory responses in mice lacking kinin B1 receptors. *ProcNatlAcadSci USA* 97:8140–8145.
- Pohl M, Stuart H, Nigam SK. 2000. Branching morphogenesis during kidney development. *Annu Rev Physiol* 62:595-620.

- Pozzi A, Coffa S, Bulus N, Zhu W, Chen D, Chen X, Mernaugh G, Su Y, Cai S, Sing A, Brissova M, and Zent R. 2006. HRas, R-Ras, and TC21 differentially regulate ureteric bud cell branching morphogenesis. *MolBiol Cell* 17:2046-2056.
- Proud D, Perkins M, Pierce JV, Yates KN, Hight PF, Herring PL, Mangkornkanok/Mark M, Bahu R, Carone F, Pisano JJ. 1981. Characterization and localization of human renal kininogen. *J BiolChem* 256:10634-10639.
- Ridley AJ, Paterson HF, Johnston CL, Diekmann D, Hall A. 1992. The small GTPbinding protein rac regulates growth factor-induced membrane ruffling. *Cell* 70:401–410.
- Ridley AJ. 2003. Cell migration: integrating signals from front to back. *Science* 302:1704-1709.
- Roman RJ, Kaldunski ML, Scicli AG, Carretero OA. 1988. Influence of kinins and angiotensin II on the regulation of papillary blood flow. *Am J Physiol-Renal Physiology* 255:F690–F698.
- Saxen L. 1987. Organogenesis of the kidney. New York: Cambridge University Press. 173 p.
- Scarpa E, Mayor R. 2016. Collective cell migration in development. *J Cell Biol* 212:143–155.
- Schachter M. 1979. Kallikreins (Kininogenases)- A group of serine proteases with bioregulatory actions. *Pharmacol Rev* 31:1-17.
- Schanstra JP, Alric C, Marin-Castaño ME, Girolami JP, Bascands JL. 1999. Renal bradykinin receptors: Localisation, transduction pathways and molecular basis for a possible pathological role (Review). *Int J Mol Med* 3:185-191.
- Schuchardt A, D'Agati V, Pachnis V, Costantini F. 1996. Renal agenesis and hypodysplasia in ret-k-mutant mice result from defects in ureteric bud development. *Development* 122: 1919-1929.
- Siragy HM. 1993. Evidence that intrarenalbradykinin plays a role in the regulation of renal function. *Am J Physiol-EndocrinolMetab* 265:E648–E654.
- Stokes JB, Grupp C, Kinne RKH. 1987. Purification of rat papillary collecting duct cells: functional and metabolic assessment. *Am J Physiol* 253:F251-262.

- Sugihara K, Nakatsuji N, Nakamura K, Nakao K, Hashimoto R, Otani H, Sakagami H, Kondo H, Nozawa S, Aiba A, et al. 1998. Rac1 is required for the formation of three germ layers during gastrulation. *Oncogene* 17:3427-3433.
- Sweeney D, Lindstrom N, Davies JA. 2008. Developmental plasticity and regenerative capacity in the renal ureteric bud/collecting duct system. *Development* 135: 2505-2510.
- Tang MJ, Cai J, Tsai SJ, Wang IK, Dressler GR. 2002. Ureteric bud outgrowth in response to RET activation is mediated by phosphatidylinositol 3-kinase. *DevBiol* 234:128–136.
- Vio C, Loyola S, Velarde V. 1992. Localization of components of the kallikrein-kinin system in the kidney: Relation to renal function. *Hypertension* 19:10-16.
- Weijer CJ. 2009. Collective cell migration in development. *J Cell Sci* 122:3215-3223.
- Wenting Z, Nelson CM. 2012. PI3K signaling in the regulation of branching morphogenesis. *BioSystems* 109:403-411.
- Xiong W, Chao L, Chao J. 1989. Renal kallikrein localization by in situ hybridization. *Kidney Int* 35:1324-1329.
- Yap AS, Kovacs EM. 2003. Direct cadherin-activated cell signaling: a view from the plasma membrane. *J Cell Biol* 160:11-16.
- Yosipiv IV, Dipp S, El-Dahr SS. 1994. Ontogeny of somatic angiotensin-converting enzyme. *Hypertension* 23:369-374.
- Yosipiv IV, Dipp S, El-Dahr SS. 1997. Role of bradykinin B2 receptors in neonatal kidney. *J Am Soc Nephrol* 6:920-928.

Figure legends

Figure 1: Effect of bradykinin (BK) on primary cultured collecting duct (CD) cells. Primary cultured CD cells were stained with FITC-coupled phalloidin to show the actin cytoskeleton. (A) Subconfluent cultured CD cells exhibit a high level of heterogeneity regarding the size of the colonies and the degree of cell association. In (B), a magnification of the region indicated in (A) is shown. Cultured CD cells with low level of cell association (C) were treated with 1 μ M BK (E). Confocal immunofluorescence images show the presence of filopodia between untreated cells (D, arrows), and the effect of BK on cell association (F). Cultured CD cells with higher level of cell association (G) were treated with 1 μ M BK (H). After BK treatment, the formation of a well-defined and continuous actin belt surrounding the colonies is evident (H). Arrows indicate actin filaments delimiting the periphery of the cell colony (E), and lamellipodia (G,H). Representative images of three experiments are shown. Scale bar and magnification: 250 μ m, 100X (A); 200 μ m, 400X (B,G,H); 200 μ m, 200X (C,E); 20 μ m, 600X (D,F).

Figure 2: Effect of BK on primary cultured CD cells by time-lapse imaging. Panels from an *in vivo* time-lapse sequence of primary cultured CD cells, imaged under differential interference contrast microscopy. The experiments were performed as described in Materials and methods. (A) CD epithelial sheet behavior before and after BK stimulation (see also Movie 1). (B) Digital magnification of a cell located in the border of the colony, showing lamellipodial dynamics before and after BK stimulation (see also Movie 2). Arrows in A and B show lamellipodia and membrane ruffle extension of marginal cells. (C) Digital magnification showing the dynamics of cell association before and after BK stimulation in a specific region of the epithelial sheet (arrows) (see also Movie 3). (D) Quantitative analysis of the size (area) of CD cell colonies expressed as percentage of control (hypothetical value of 100%, non-significant p value), and error bars represent

SEM. Representative images of three experiments are shown. Scale bar and magnification: 20 μm for all panels, 600X.

Figure 3: Mechanism of action of BK on primary cultured CD cells. Subconfluent cultured CD cells were pretreated either with 100 nM of the B2R antagonist HOE-140 for 30 min before 1 μM BK stimulation for 1 min or with 10 μM of the PI3K inhibitor LY294002 for 10 min before 1 μM BK stimulation for 1 min. Cells were stained with FITC-coupled phalloidin. Wide-field fluorescence microscopy showing untreated cells (A) and the effect of BK on cell association (D), the effect of HOE-140 (B) and LY294002 (G) before BK stimulation on cell association (E,H). Confocal immunofluorescence image showing HOE-140-treated cells (C,F) and LY294002-treated cells (I). Insert in H shows the decreased number of filopodia between cells. Representative images of three experiments are shown. Scale bar and magnification: 200 μm , 400X (A, B, D, E, G, H), and 20 μm , 600X (C, F, I). HOE: HOE-140, LY: LY294002.

Figure 4: Effect of BK B2R antagonist and PI3K inhibitor on primary cultured CD cells by time-lapse imaging. Panels from an *in vivo* time-lapse sequence of primary cultured CD cells imaged under phase contrast microscopy. The experiments were performed as described in Materials and methods. Behavior of the CD epithelial sheet before and after HOE-140 (A) or LY294002 pretreatments (B), and BK stimulation (see also Movies 4 and 5). (C) Quantitative analysis of the size (area) of CD cell colonies expressed as percentage of control (hypothetical value of 100%, non-significant p value), and error bars represent SEM. Representative images of three experiments are shown. Scale bar and magnification: 200 μm for all panels, 400X. HOE: HOE-140, LY: LY294002.

Figure 5: PIP3 and PIP2 distribution in cultured CD cells after BK stimulation. Subconfluent cultured CD cells were pretreated either with 1 μM BK for 1 min or with the B2R antagonist HOE-140 (100 nM) before 1 μM BK stimulation for 1 min. Cells were immunostained with an antibody

against PIP2 (red) and against PIP3 (green), and the nuclei were stained with Hoechst (blue). The images correspond to untreated cells (A), cells stimulated with BK (C), HOE-Control (E), and HOE-BK (G). The respective overlay images are shown in the right column. Quantitative analysis of the number of PIP3-positive CD cells expressed as percentage and error bars represent SEM. Unpaired t-test: C vs BK, $p=0.02$, and HOE-C vs HOE-BK, non-significant p value. Representative images of three experiments are shown. Scale bar and magnification: 200 μm , 400X. HOE: HOE-140

Figure 6: BK-induced phosphorylation of Akt in CD cultured cells. Immunoblot analysis of Akt (A) and p-Akt (Thr 308) (B) content in protein lysates from primary cultured CD cells in response to 1 μM BK for 5 min and the indicated inhibitors. Equal amounts of protein were loaded in each lane. Protein loading was controlled by staining with Coomassie blue. Results are expressed as percentage of control (hypothetical value of 100%) and error bars represent SEM. (*) $p < 0.05$. Results correspond to a representative experiment of three individual assays. HOE: HOE-140, LY: LY294002.

Figure 7: p-Akt distribution in cultured CD cells after BK stimulation. Subconfluent cultured CD cells were incubated with 1 μM BK for 5 min. Cells were immunostained with an antibody against Akt and p-Akt (Thr 308). The images correspond to untreated cells (A, C) and cells stimulated with BK (B,D). Arrows in B show p-Akt localization in the membrane of some cells of the edge of the colony. (E-F) The pixel intensity profile of the fluorescence of Akt (E) and p-Akt (F) was assessed starting at the cell edge toward the nucleus for each time-point of BK stimulation to study the intracellular localization of both proteins. Values are means \pm SEM. Representative images of three experiments are shown. Scale bar and magnification: 200 μm , 400X.

Figure 8: PCNA and p38 MAPK expression in cultured CD cells after BK stimulation. Subconfluent cultured CD cells were treated with 1 μM BK for 1 min. Cells were immunostained

with an antibody against PCNA (green), and the nuclei were stained with Hoechst (blue). The images correspond to untreated (A, B), and BK-treated cells (C,D). In the left column, the phase contrast and Hoechst overlay images are shown. Quantitative analysis of the number of PCNA-positive CD cells are expressed as percentage, and error bars represent SEM. Unpaired t-test: C vs BK, $p=0.0001$. Representative images of three experiments are shown. Scale bar and magnification: 200 μm , 400X. Immunoblot analysis of PCNA (E) and phosphorylated-p38 MAPK (Thr180/Tyr182) (F) content in protein lysates from primary cultured CD cells in response to 1 μM BK for 5 min and the indicated inhibitor. Equal amounts of protein were loaded in each lane. Protein loading was controlled by staining with Coomassie blue. Results are expressed as percentage of control (hypothetical value of 100%) and error bars represent SEM. Unpaired t-test: PCNA: C vs BK, $p= 0.0005$; LY-C vs LY-BK, $p= 0.0001$. p38 MAPK: C vs BK, $p= 0.004$; LY-C vs LY-BK, $p= 0.0001$. Results correspond to a representative experiment of three individual assays. LY: LY294002.

Figure 9: Rac1 expression and distribution in cultured CD cells after BK stimulation.

Subconfluent cultured CD cells were pretreated either with the B2R antagonist HOE-140 (100 nM) before 1 μM BK stimulation for 1 min or with the PI3K inhibitor LY294002 (10 μM) before 1 μM BK stimulation for 1 min. Cells were immunostained with an antibody against Rac1 (green), and the nuclei were stained with Hoechst (blue). The respective overlay images are shown in the right column. The images correspond to untreated cells (A-C), cells stimulated with BK (D-F), HOE-Control (G-I), HOE-BK (J-L), LY294002-Control (M-O), and LY294002-BK (P-R). The images shown in the left column correspond to the respective phase contrast microscopy images. Quantitative analysis of the number of Rac1-positive CD cells expressed as percentage and error bars represent SEM. Unpaired t test with Welch correction: C vs BK, $p=0.01$; and unpaired t-test: HOE-C vs HOE-BK, non-significant p value; LY-C vs LY-BK, non-significant p value.

Representative images of three experiments are shown. Scale and magnification: 200 μm , 400X.
HOE: HOE-140, LY: LY294002.

Figure 10: Ret expression in cultured CD cells after BK stimulation. Subconfluent cultured CD cells were treated with 1 μM BK for 1 or 5 min. Wide-field fluorescence microscopy images showing the expression of Ret and DBA staining. Cells were stained with the lectin DBA (red) and with a specific anti-Ret antibody (green), counterstained with Hoechst 33258 (blue). The respective overlay images are shown in the right column. Quantitative analysis of the number of Ret-positive CD cells is expressed as percentage, and error bars represent SEM. Tukey-Kramer test: C vs BK 1 min, and C vs BK 5 min, $p=0.001$; BK 1 min vs BK 5 min, non-significant p value. Representative images of three experiments are shown. Scale bar and magnification: 20 μm , 600X

Figure 11: Evolution of B2R expression during successive stages of primary cultured CD cells. CD cells were cultured for the indicated times (A-L). CD cells isolated from renal papillae of adult rats were cultured for 96 h (M-O). Wide-field fluorescence microscopy images showing the evolution of B2R expression and DBA from the initial stage of culture (1 h after cell plating). Cells were stained with the lectin DBA (red) and with a specific anti-B2R antibody (green), counterstained with Hoechst 33258 (blue). Digital magnifications shown in the left column represent the merged images corresponding to the inserts. Arrows in C, I, L and O show B2R-positive cells. Representative images of three experiments are shown. Scale bar and magnification: 100 μm for all panels, 400X. B2R: bradykinin B2 receptor.

Figure 12: Analysis of B2R expression, DBA staining and E-cadherin distribution in primary cultured CD cells. Primary cultured CD cells were stained with the lectin DBA (red) and with anti-E-cadherin antibody (green) (A-C), with anti-E-cadherin (green) and anti-B2R antibodies (red) (D-F). Wide-field fluorescence microscopy showing the distribution of E-cadherin and DBA staining (A-C), E-cadherin and B2R (D-F). Arrows in F show B2R-positive cells. 3D reconstruction of

Accepted Article

confocal images (G) and xz-planes of cells stained with anti-E-cadherin (red) and anti-B2R antibodies (green). (G`) Digital magnification of the region indicated in G. The analysis of xz planes shows the distribution of E-cadherin and B2R. Scale bar and magnifications: 100 μm , 20X (A-C); 100 μm , 40X (D-F).

Figure 13: Analysis of E-cadherin distribution in cultured CD cells after BK stimulation.

Subconfluent cultured CD cells were either incubated with 1 μM BK for 1 or 5 min (C,E) or pretreated with the B2R antagonist HOE-140 (100 nM) before 1 μM BK for 1 or 5 min (D,F). Cells were immunostained with anti-E-cadherin antibody. Inserts in A, C, and E show a digital magnification of the lateral membrane at cell-cell contacts. Scale bar and magnifications: 100 μm , 40X. BK: bradykinin, B2R: bradykinin B2 receptor, HOE: HOE-140.

Figure 14: Analysis of β -catenin distribution in cultured CD cells after BK stimulation.

Subconfluent cultured CD cells were either incubated with 1 μM BK for 1 min (B) or pretreated with the B2R antagonist HOE-140 (100 nM) before 1 μM BK stimulation for 1 min (F). Cells were immunostained with anti- β -catenin antibody. (C,D) Digital magnification of the region indicated in A and B. Scale bar and magnifications: 100 μm , 40X. BK: bradykinin, B2R: bradykinin B2 receptor, HOE: HOE-140.

Figure 15: Signaling pathways involved in BK action in CD cells during renal postnatal development. The mechanism by which BK induces cell compaction and favors the collective migration of epithelial colonies of CD would be mediated by the activation of the PI3K and its downstream Akt and Rac1 pathways as a result of binding to its B2 receptor. PI3K would constitute a point of convergence of the signaling pathway activated by BK/B2R and GDNF/Ret.

Supplemental material

Text for both the electronic and the print version for the portions of the article that refer to this content.

BK favors CD cell association to form migratory colonies through B2R activation

To investigate the *in vivo* behavior of cultured CD cells before and after BK stimulation, we performed time-lapse experiments. CD cells cultured for 19 to 24 h were maintained on a heated platform (37°C) and imaged either under differential interference contrast (DIC) with an oil immersion 60X objective or under phase contrast with a 40X objective (air). A CD cell colony was randomly selected and images were captured every 20 seconds for 1 h 26 min. BK (final concentration 1 μ M) was added to the culture at 34 min 20 sec, and the behavior of the cultured CD cells was analyzed before and after BK stimulation. When experiments were performed in the presence of the B2R antagonist HOE-140 (100 nM), cells were preincubated for 30 min before BK stimulation, whereas when they were performed in the presence of LY294002 (10 μ M), cells were preincubated for 20 min before BK stimulation. Images were captured every 20 seconds for 86 min and 73 min, respectively. After image acquisition, the movies were generated using the Image J free software. As apparent from the time-lapse videos, a group of CD cells behaved as a collective migratory unit, exhibiting an important protrusive activity. At any given time, many marginal cells were extending lamellipodia in all directions. During the recording, the cells remained closely attached, without losing their contacts with other cells (Movie 1). After adding BK, a prominent increase was observed in the rate of lamellipodia and membrane ruffle extension of marginal cells (Movie 2). We also noticed that, after BK stimulation, some cells appeared to physically embed their plasma membrane into the adjacent cell membrane. Thereafter, a continuous line was formed, denoting cell-cell adhesion (Movie 3). Our results suggest that BK induces and maintains cell-cell association without any discontinuity in the monolayer, thus favoring the collective cell motility of the CD cells.

Movie 1: Behavior of cultured CD cells before and after BK stimulation. Protrusive activity is visible at any given time, supporting the notion that CD cells behave as a collective migratory unit. After adding BK, a prominent increase was observed in the rate of lamellipodia and membrane ruffle extension of cells. This movie corresponds to the images shown in Fig. 2A.

Movie 2: Lamellipodial dynamics of a CD cell colony. Detail of the lamellipodial dynamics of a cell located in the margin of the CD cell colony before and after BK stimulation. Although the cell extends lamellipodia at any given time, a notorious increase was observed in the size of lamellipodia and rate of lamellipodia formation after BK stimulation. This movie corresponds to the images shown in Fig. 2B.

Movie 3: BK-induced CD cell association. Detail of the establishment of cell-cell adhesion before and after BK stimulation. Note the formation of a continuous line between the cells located in the upper corner of the recorded field, denoting cell-cell adhesion. This movie corresponds to the images shown in Fig. 2C.

Movie 4: BK-induced CD cell compaction depends on B2 receptor stimulation. Although the lamellipodial extension was not affected by the treatment with HOE-140 or even after BK stimulation, the BK-induced cell compaction and the membrane ruffling process were completely prevented by the addition of the B2R antagonist. This movie corresponds to the images shown in Fig. 4A.

Movie 5: PI3K is required for lamellipodial extension and peripheral ruffling in a CD cell colony. The lamellipodial extension was suppressed after LY294002 incubation, and the addition of BK did not affect the rate or length of these cytoskeletal protrusions. This movie corresponds to the images shown in Fig. 4B.

Figure 1

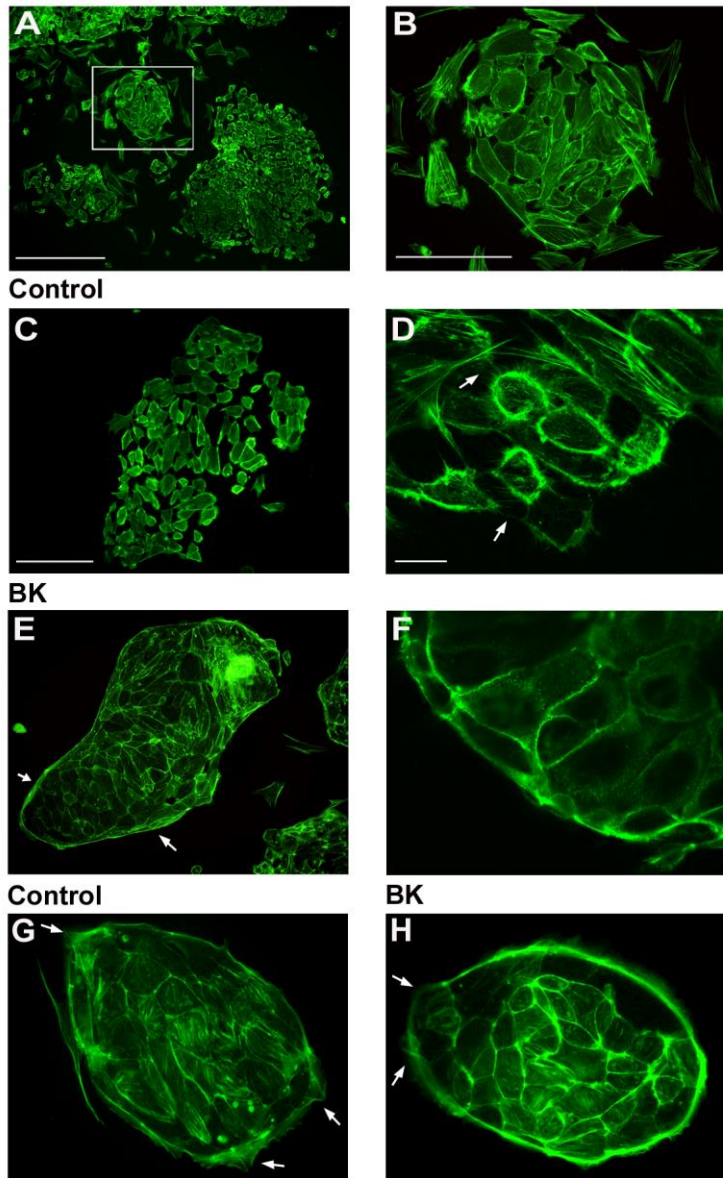


Figure 2

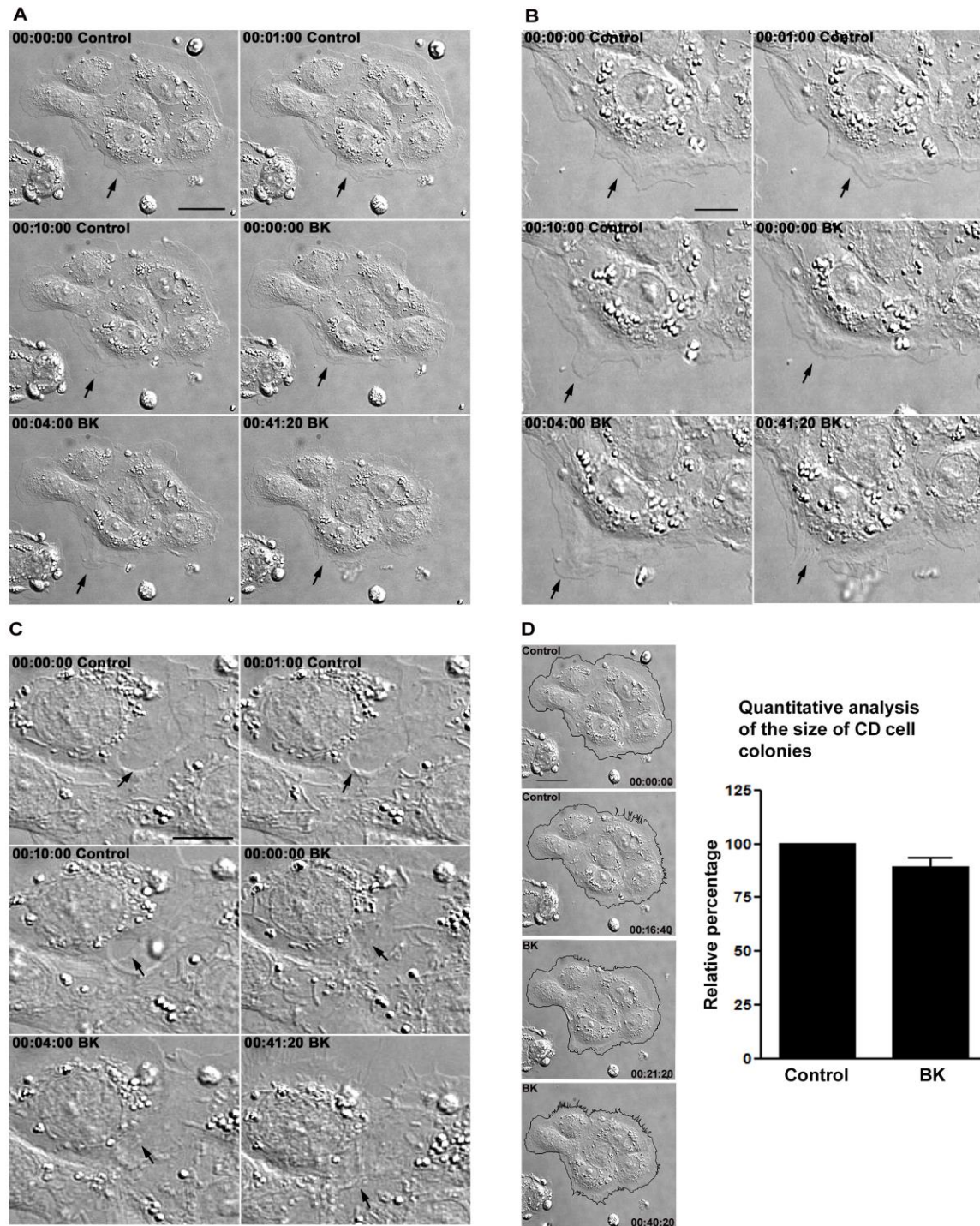


Figure 3

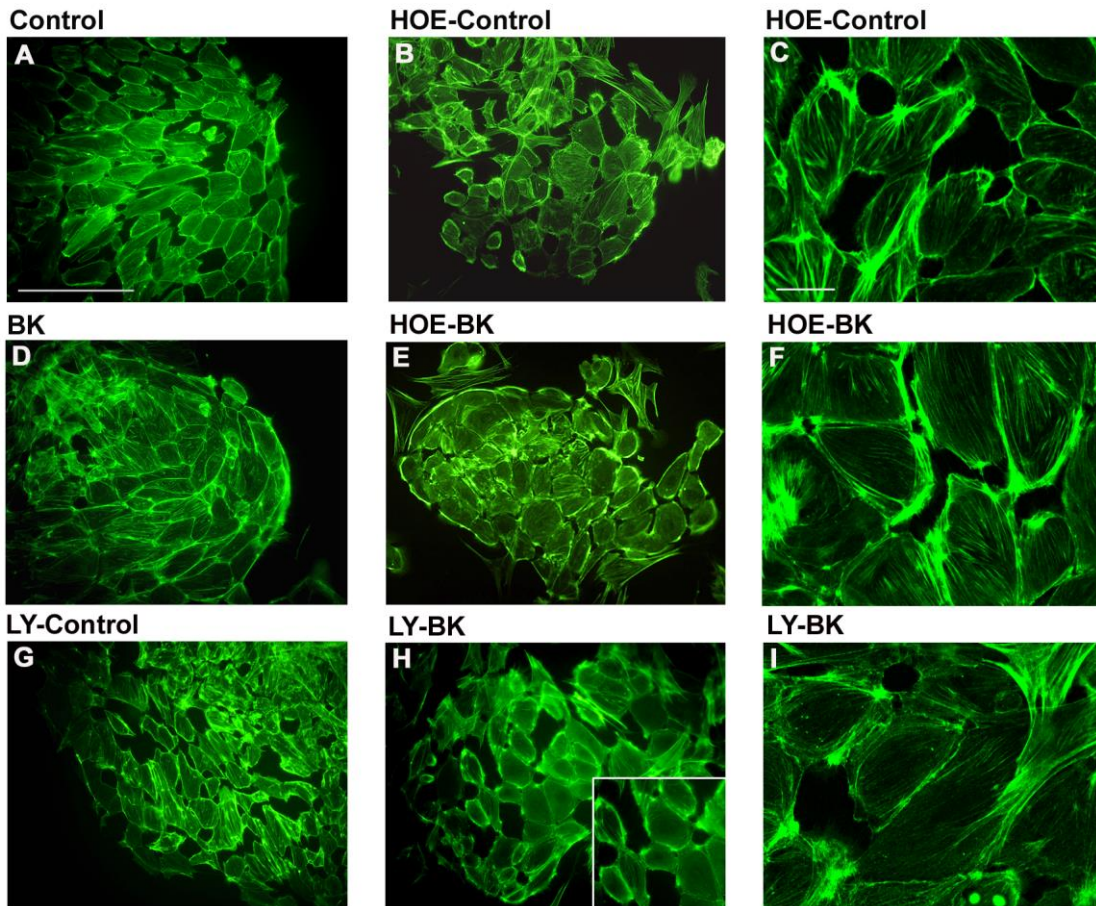


Figure 4

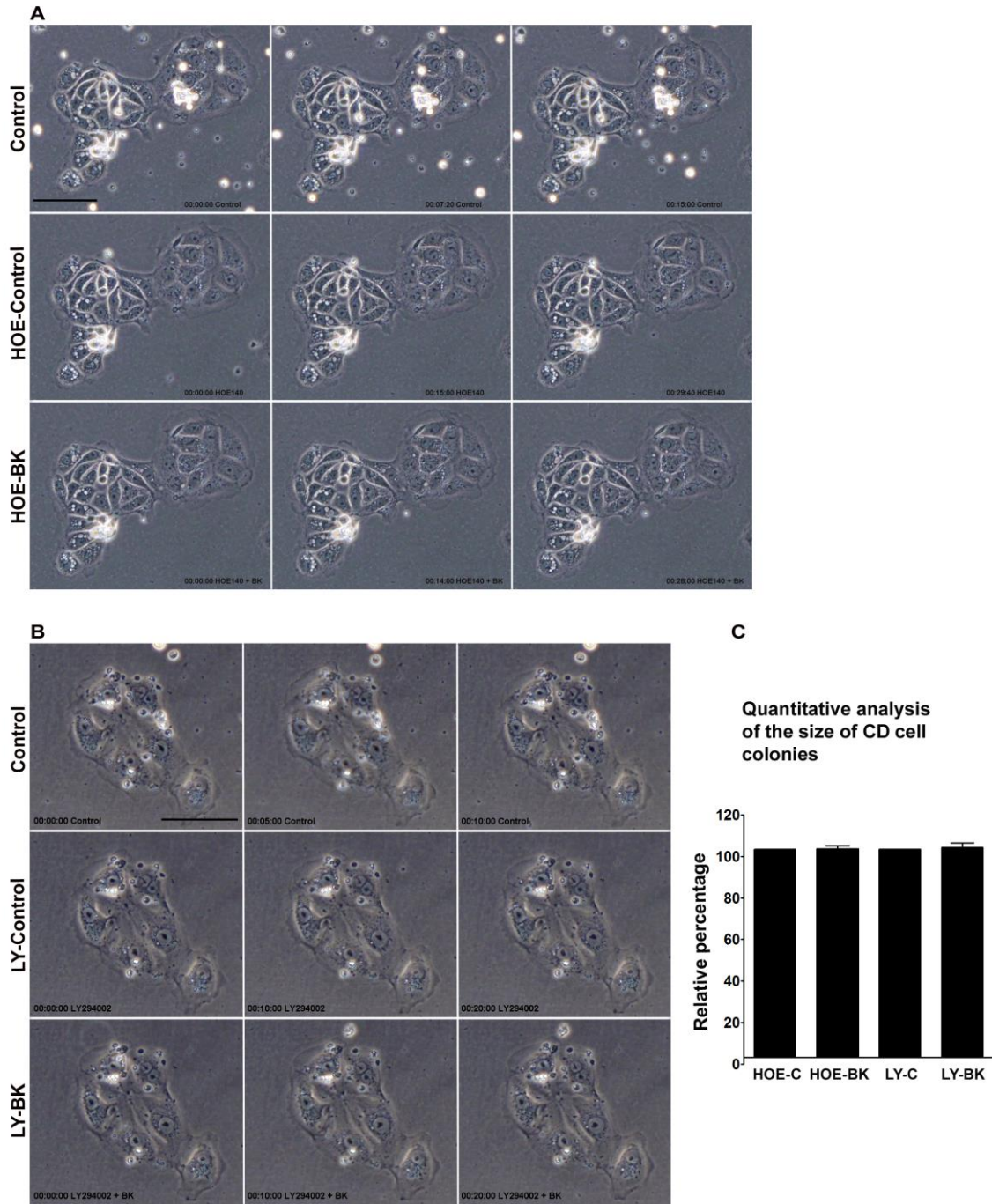


Figure 5

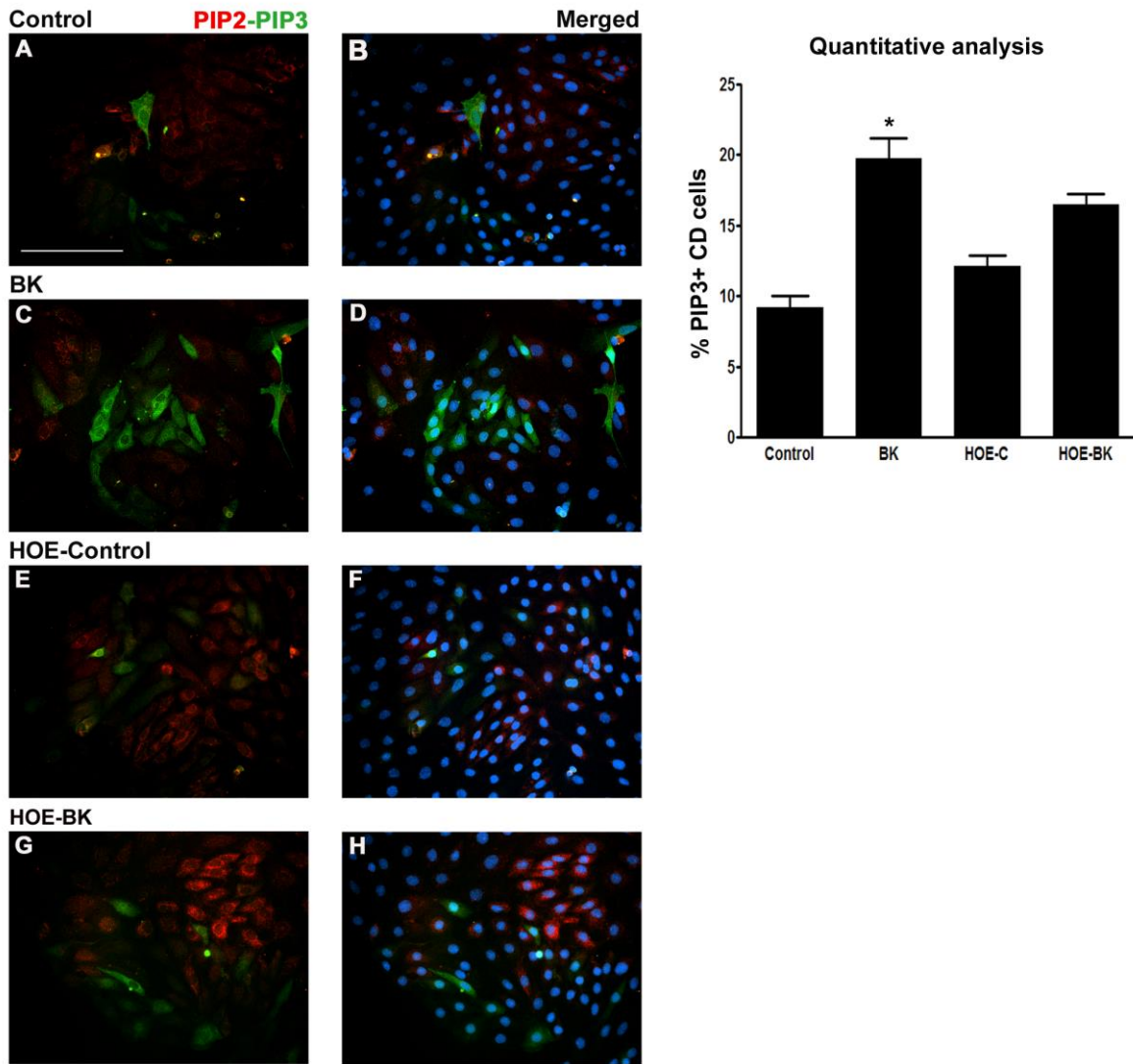


Figure 6

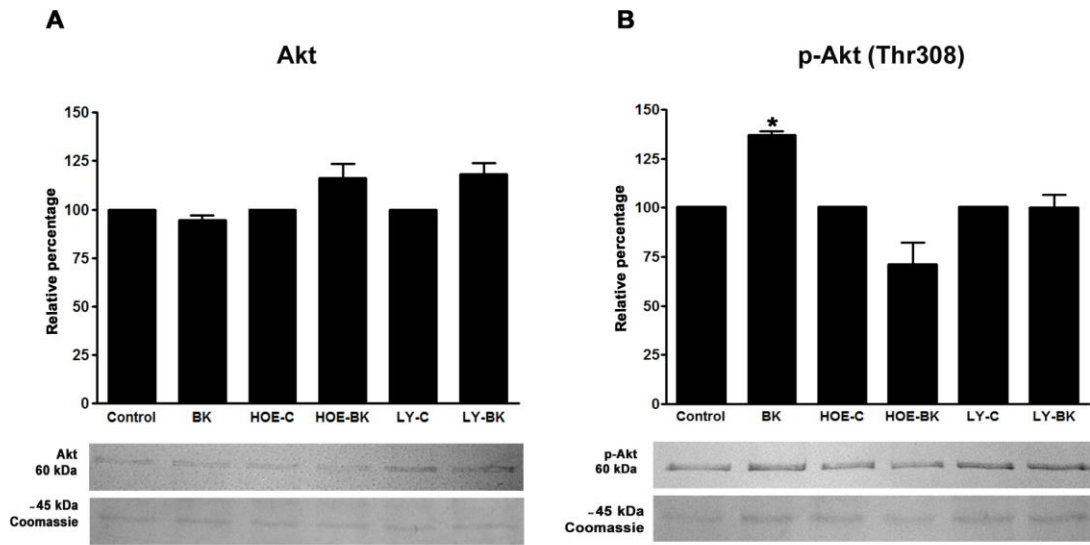


Figure 7

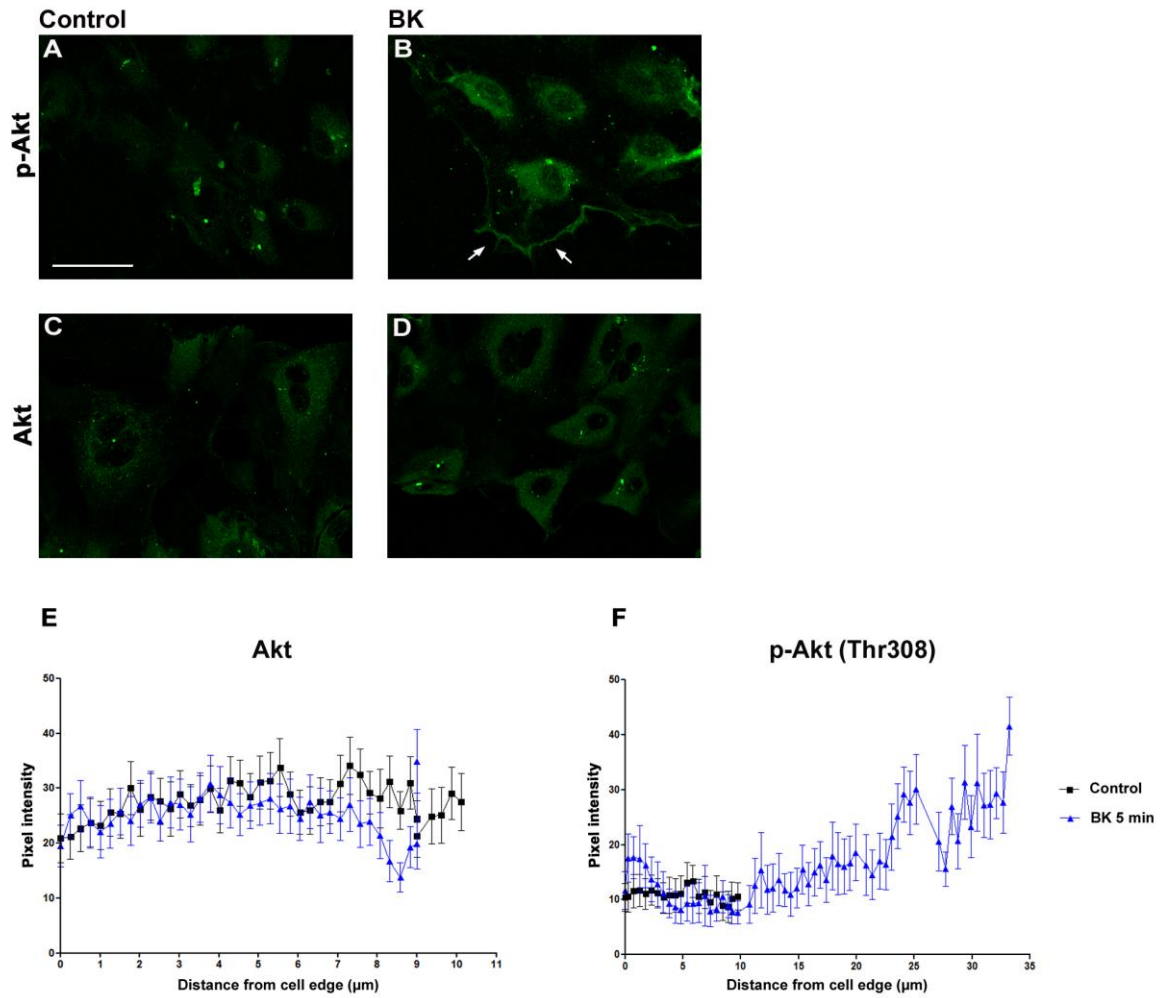


Figure 8

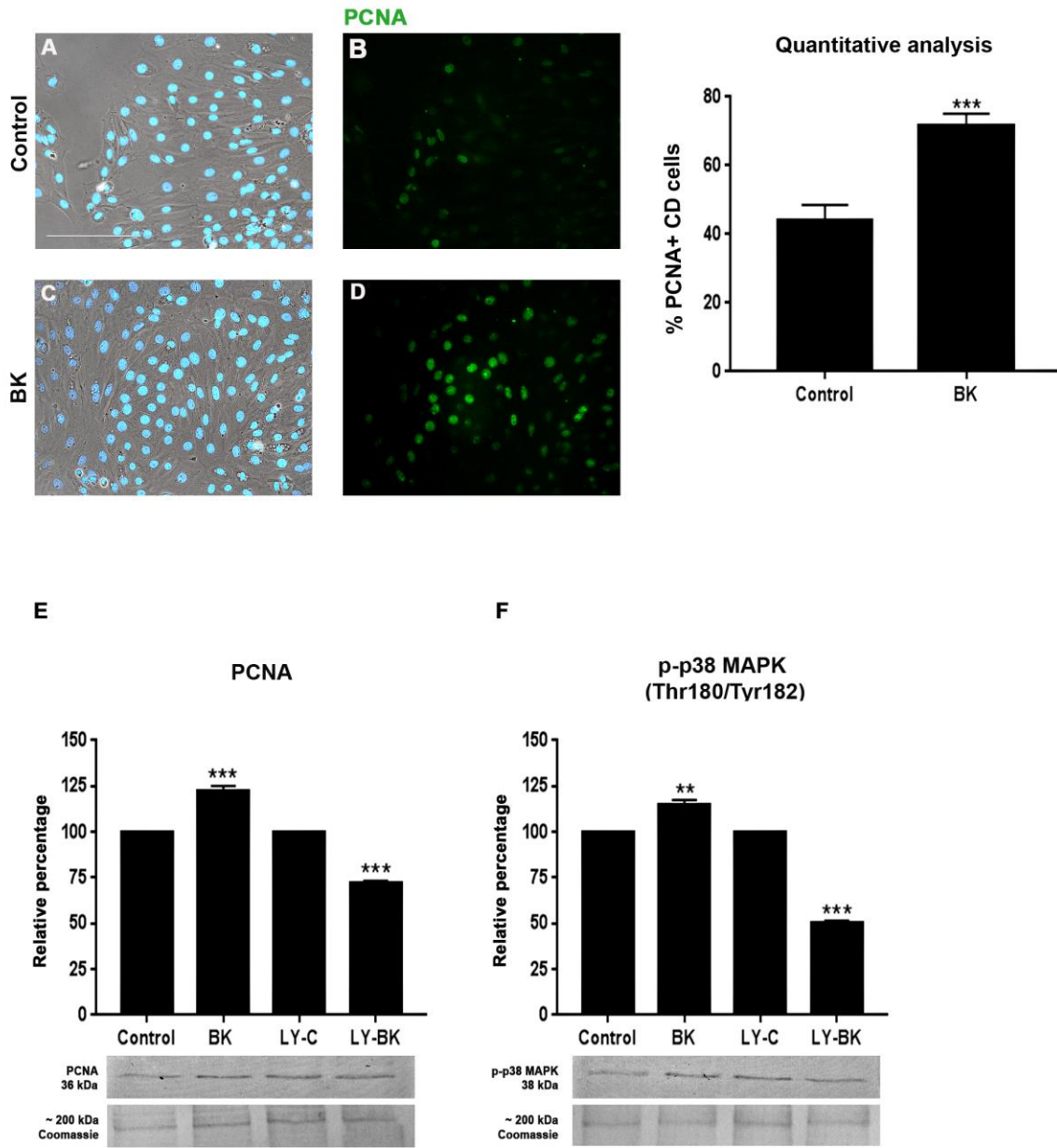


Figure 9

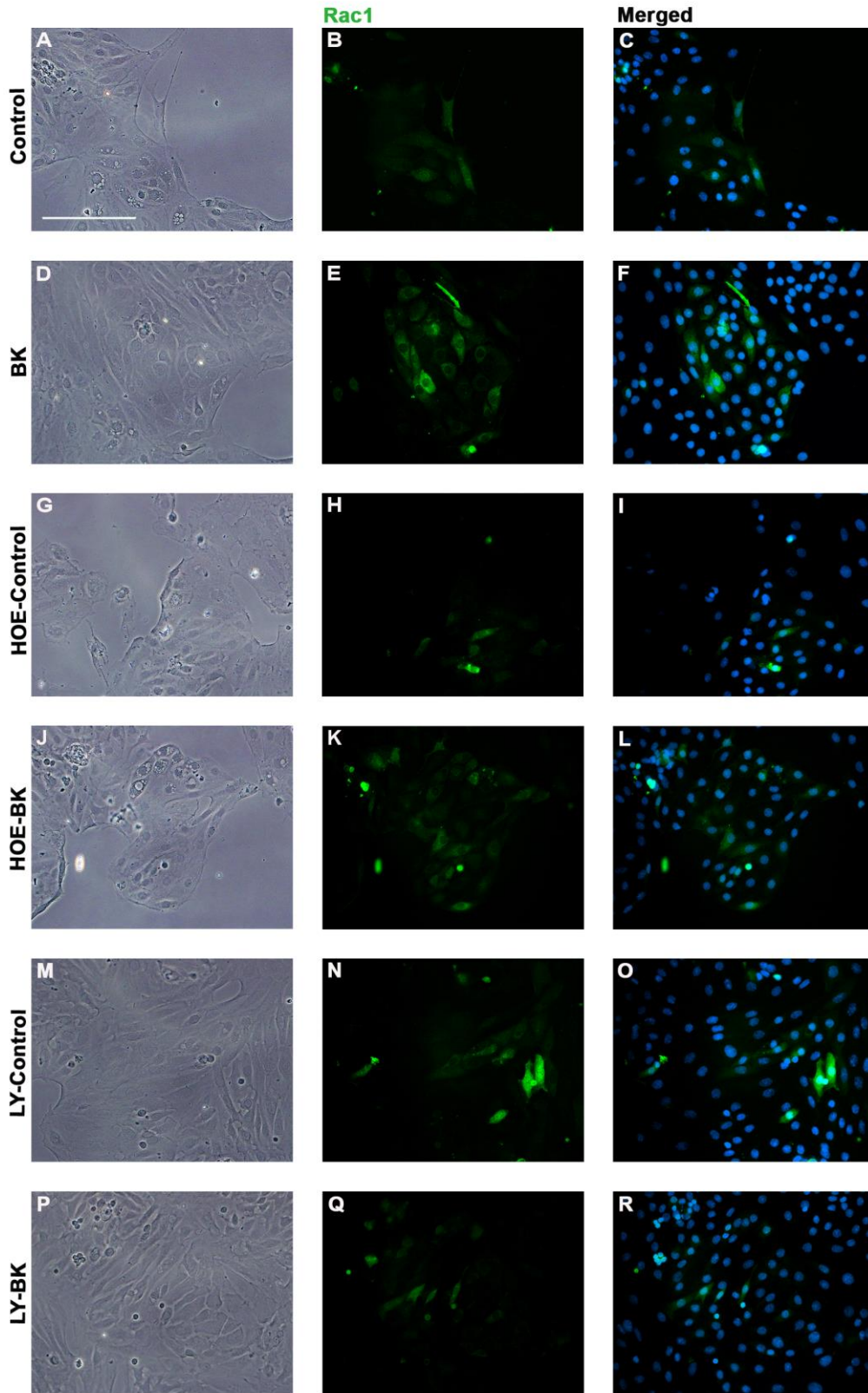


Figure 9 (cont.)

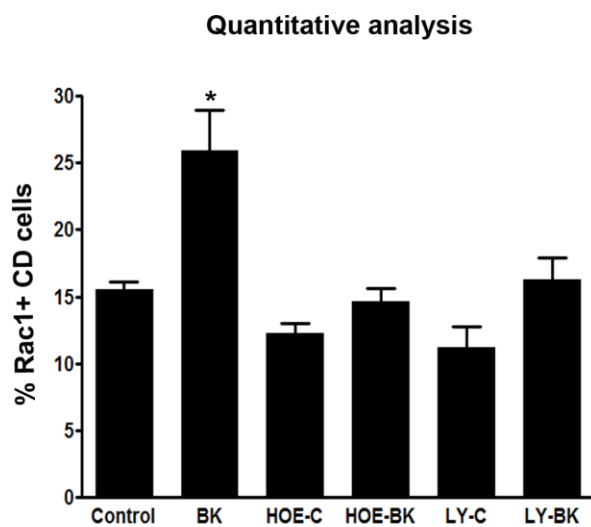


Figure 10

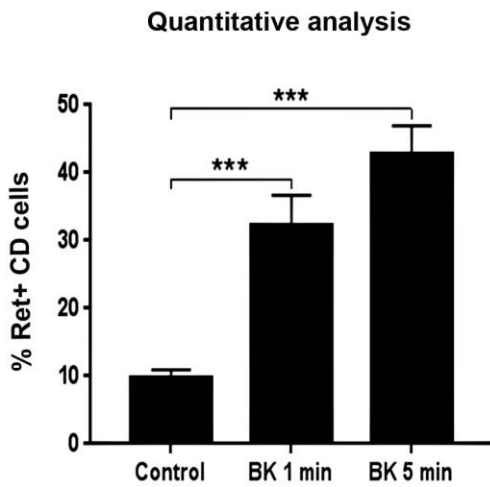
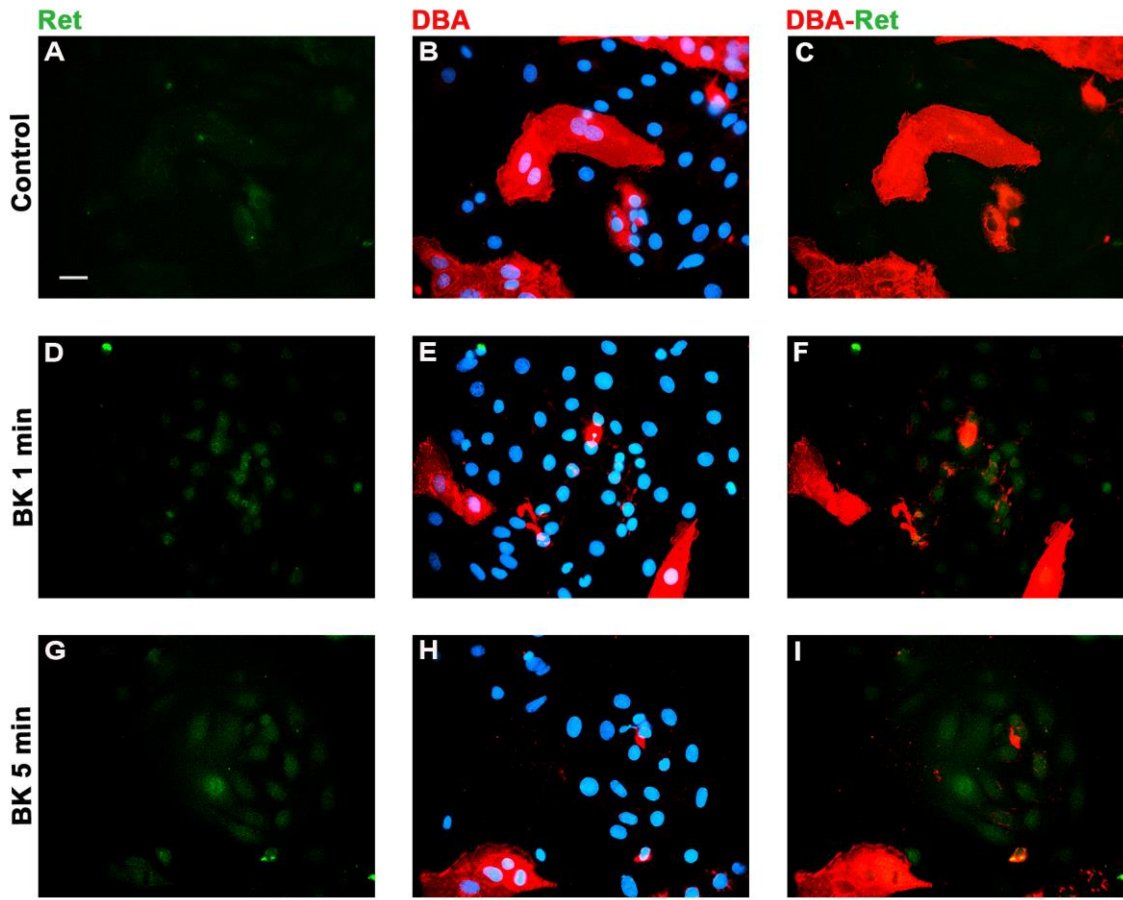


Figure 11

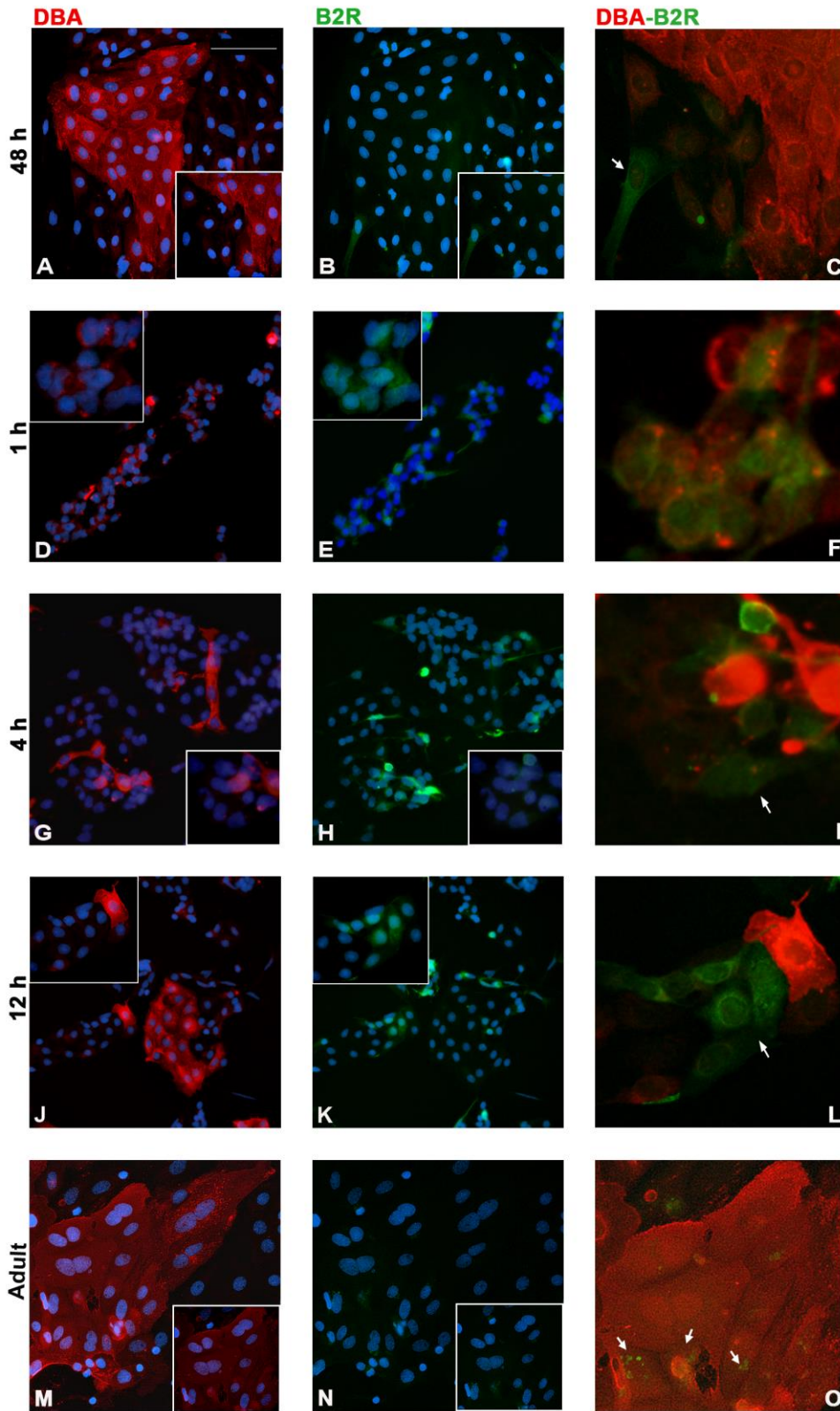


Figure 12

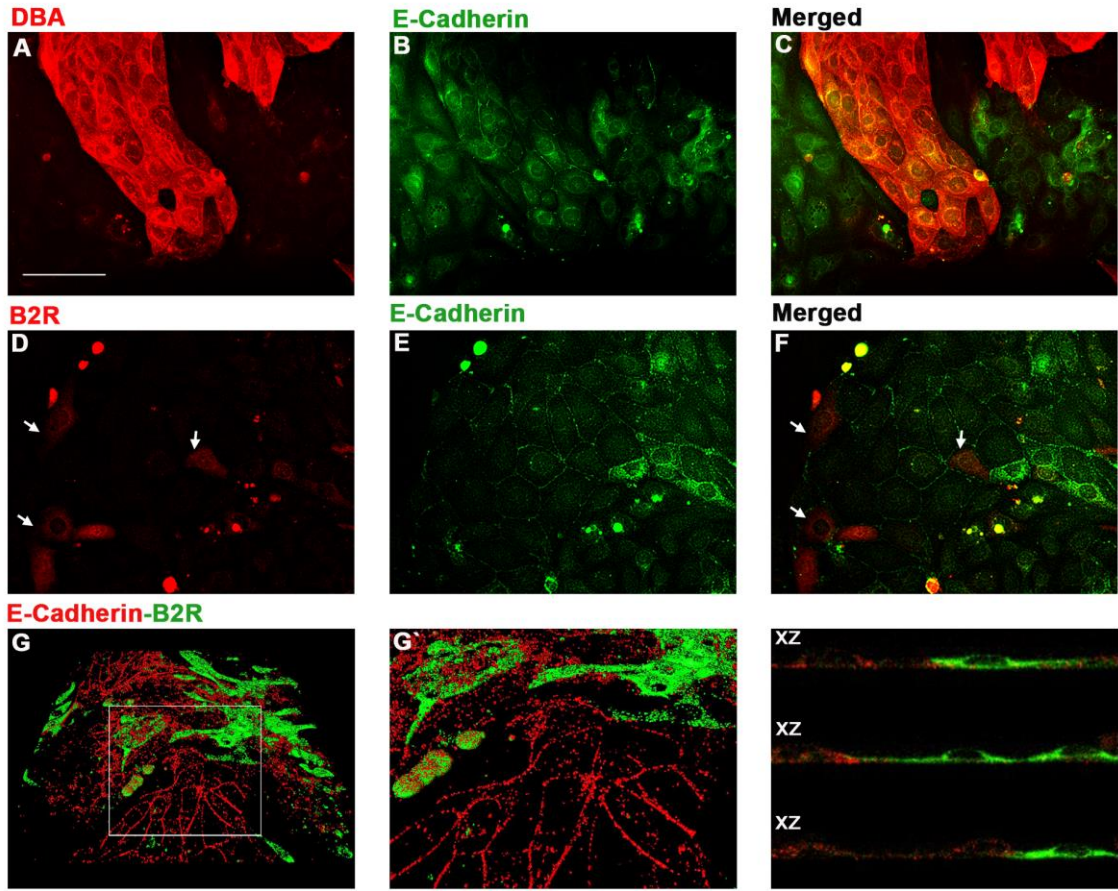


Figure 13

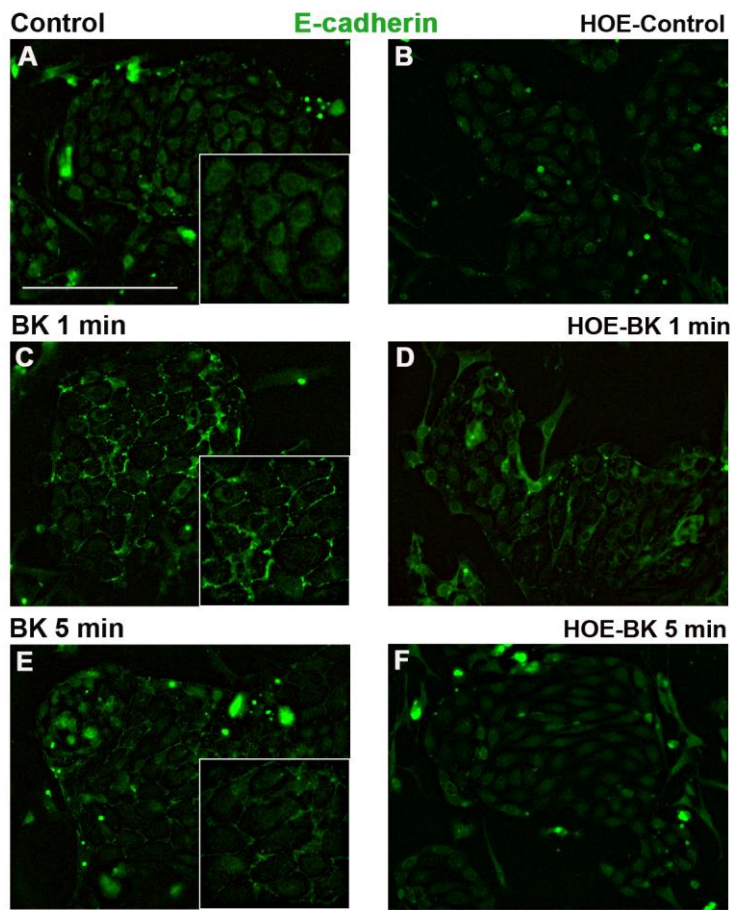


Figure 14

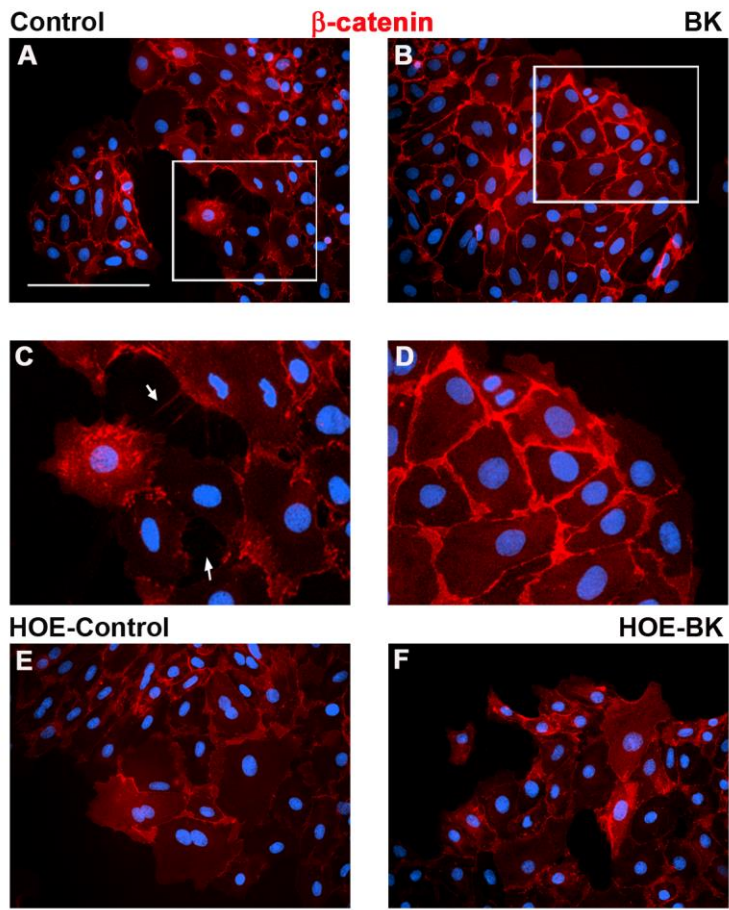


Figure 15

